5961: ASTRONOMICAL FORCING

ELEMENTS OF ORBITAL GEOMETRY:

1. ORBITAL ELLIPSE

$$\text{ECCENTRICITY (e)} = \frac{(a^2 - b^2)^{0.5}}{a}$$

where a = semi-major axis of ellipse
b = semi-minor axis

e varies from 0 to 0.06; currently e = 0.0167
10 ka e = 0.019

RADIUS VECTOR, $\rho = r / \bar{r}$
(Sun's distance)

$$\rho = (1 - e^2) / (1 + e \cos \upsilon)$$

where υ = angle between perihelion and longitiude of vernal equinox

ρ varies from (1-e) to (1+e) : 0.94 - 1.06

Today, angle between perihelion (4 Jan) and vernal Equinox (22 March) is 78°

Period of υ is 21 ka.

CALORIC WINTER / SUMMER : TIME THAT EARTH SPENDS IN WINTER AND SUMMER (DEFINED BY ORBIT)

$$(\tau_s - \tau_w) = \frac{4\varepsilon}{\pi}(365)\sin\upsilon$$

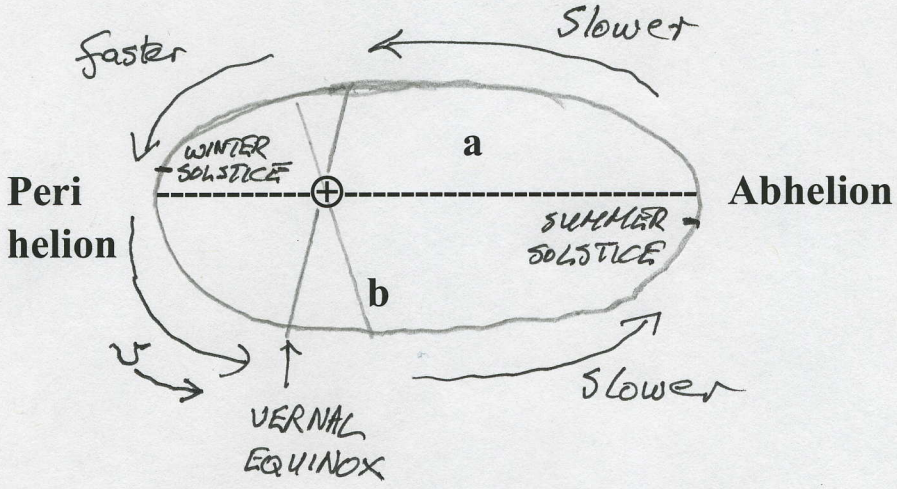

Currently $(\tau_s - \tau_w) = 7.5$
(i.e. NH winter 7.5 days < NH summer

Seasonal ∂T varies up to ± 20 days

Eccentricity

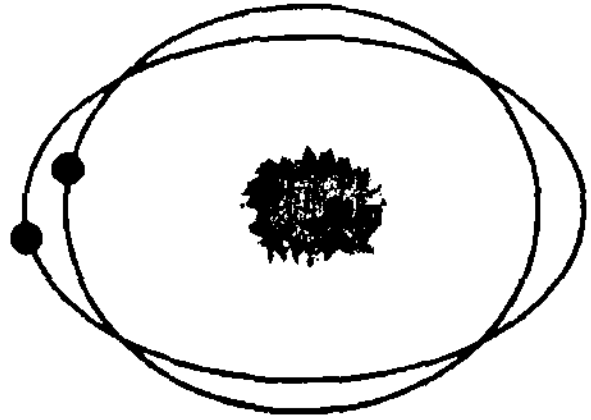

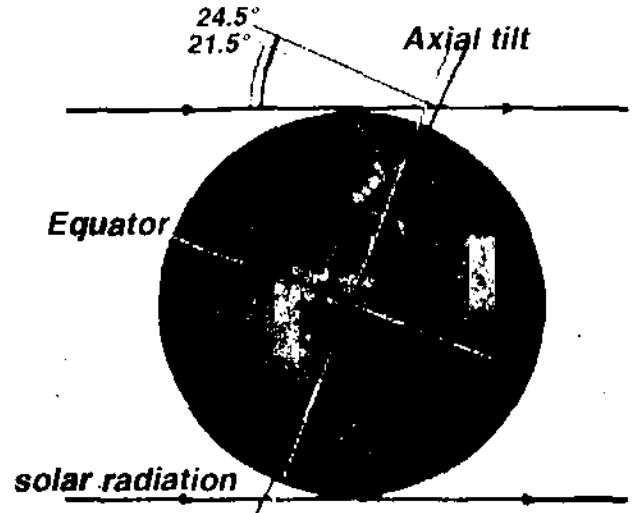

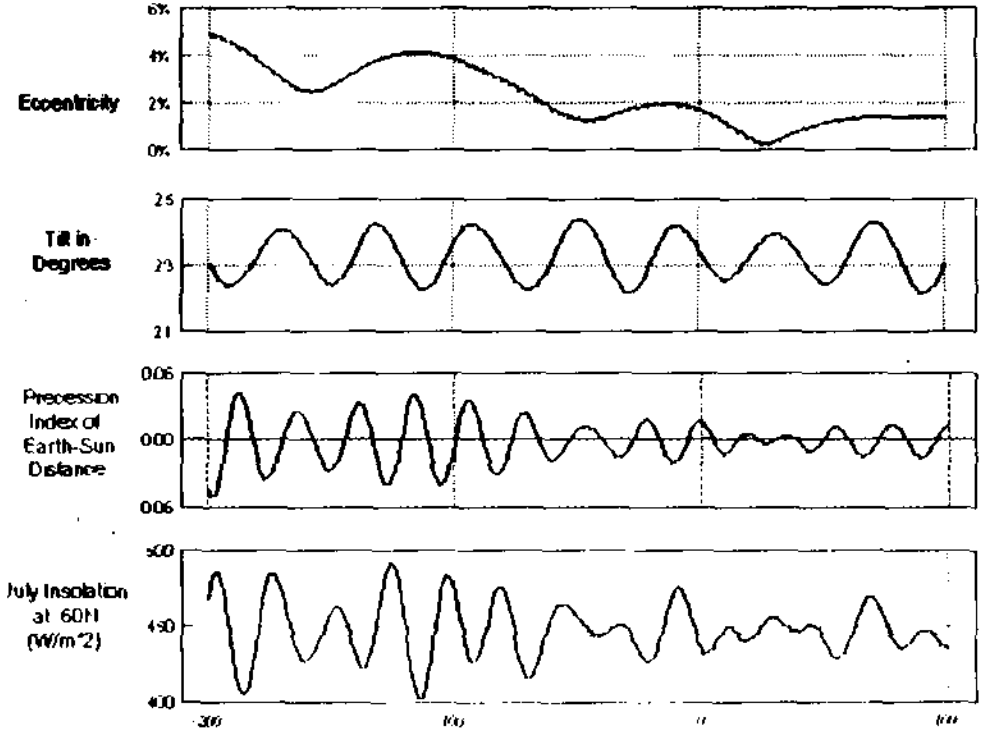

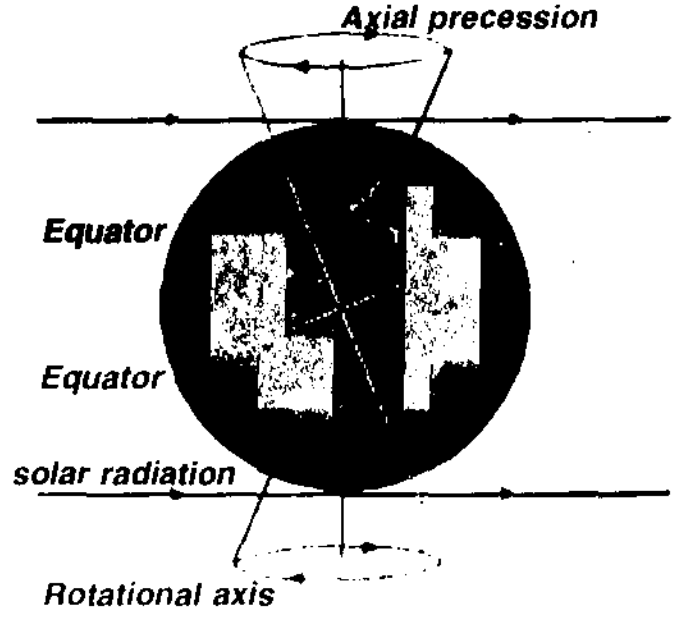

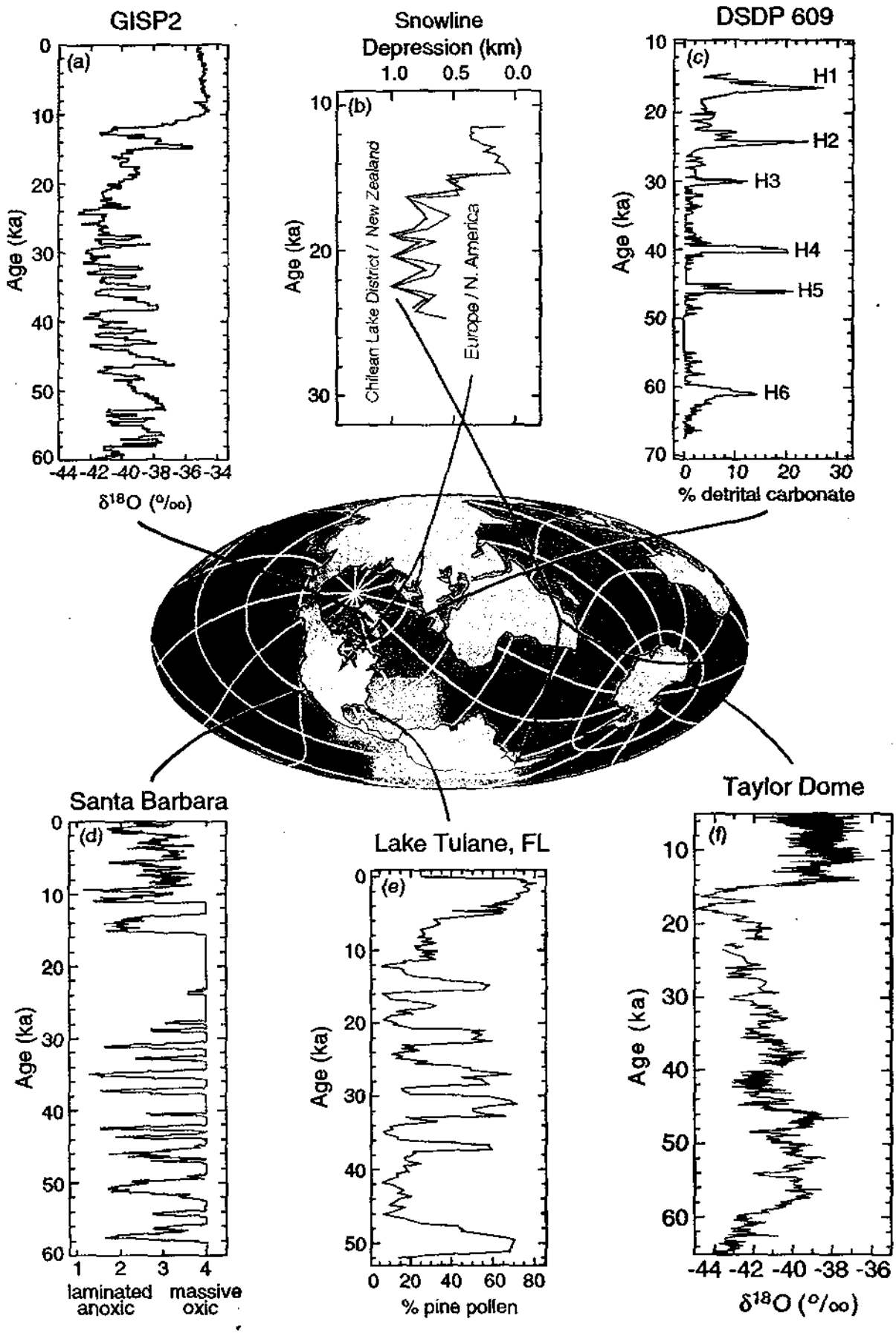
GISP2
(a)
Age (ka)
δ18O (‰)
Snowline
Depression (km)
(b)
Chilean Lake District / New Zealand
Europe / N. America
DSDP 609
(c)
H1
H2
H3
H4
H5
H6
% detrital carbonate
Santa Barbara
(d)
laminated anoxic
massive oxic
Lake Tulane, FL
(e)
% pine pollen
Taylor Dome
(f)
δ18O (‰)

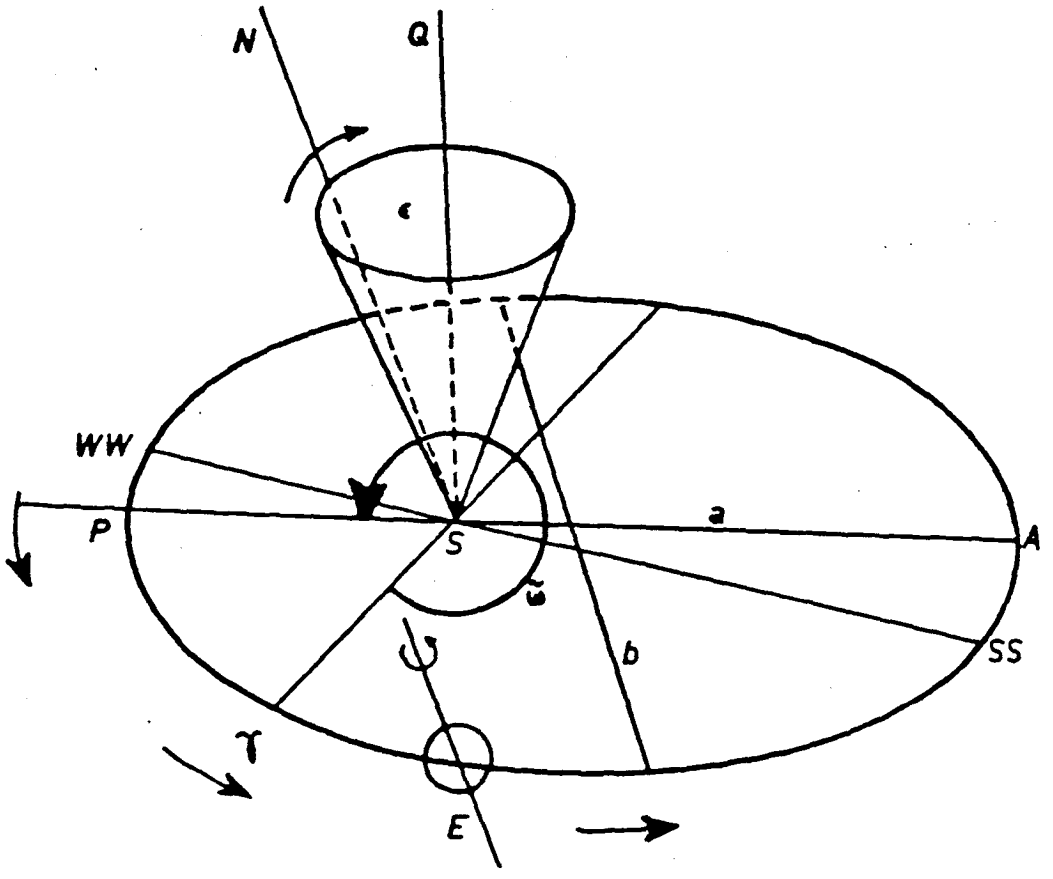

Figure 1 Elements of the earth's orbit. The orbit of the Earth, E, around the Sun S is represented by the ellipse P γ E A, P being the perihelion and A the aphelion. Its eccentricity, e, is given by $(a^2-b^2)^{1/2}/a$, a being the semimajor axis and b the semiminor axis. WW and SS are respectively the winter and the summer solstice, γ is the vernal equinox ; WW, SS and γ are located where they are today. SQ is perpendicular to the ecliptic and the obliquity, ε, is the inclination of the equator upon the ecliptic, i.e. ε is equal to the angle between the earth's axis of rotation SN and SQ. $\tilde{\varpi}$ is the longitude of the perihelion relatively to the moving vernal equinox and is equal to $\Pi+\psi$. The annual general precession in longitude, ψ, describes the absolute motion of γ along the earth's orbit relative to the fixed stars. Π, the longitude of the perihelion, is measured from the reference vernal equinox of 1950 A.D. and describes the absolute motion of the perihelion relatively to the fixed stars. For any numerical value of $\tilde{\varpi}$, 180° is substracted for a practical purpose : observations are made from the Earth, and the Sun is considered as revolving around the Earth.

SOLAR RADIATION AT SURFACE (no atmosphere)

$S = S_o \cos z$, where z = zenith angle)

$\cos z = \sin \varphi \sin \delta + \cos \varphi \cos \delta \cos H$

ϕ = latitude δ = declination (Lat. where 90° sun at noon)
H = hour angle [15°(12 – t)], t = local solar time

S integrated from sunrise to sunset: $dt = (\tau / 2\pi)\, dH$

$$\int_{\text{Sunset}}^{\text{Sunrise}} S\, d\tau = \int_{0}^{\pi/2} \tau / \pi \left[\left(\frac{S_o}{\rho^2} \right) (\cos z) \right] dH$$

Periods for ρ^2 are 413, 95, 123 and 100 Ka

The annual change in S_o for $\Delta\rho$ is 6.5%
Seasonal change is 24%

2. AXIAL TILT- OBLIQUITY OF THE ECLIPTIC (ε)

CAUSED BY 'PULL' OF SUN AND MOON ON THE EQUATORIAL BULGE OF THE GEOID.

TILT OF AXIS CAUSES DECLINATION ANGLE. δ, TO VARY BETWEEN 22° AND 24.5° (NOW 23.5°)
41 KA period

MAJOR EFFECT IN HIUGH LATITUDES) AND EQUATOR-POLE GRADIENTS

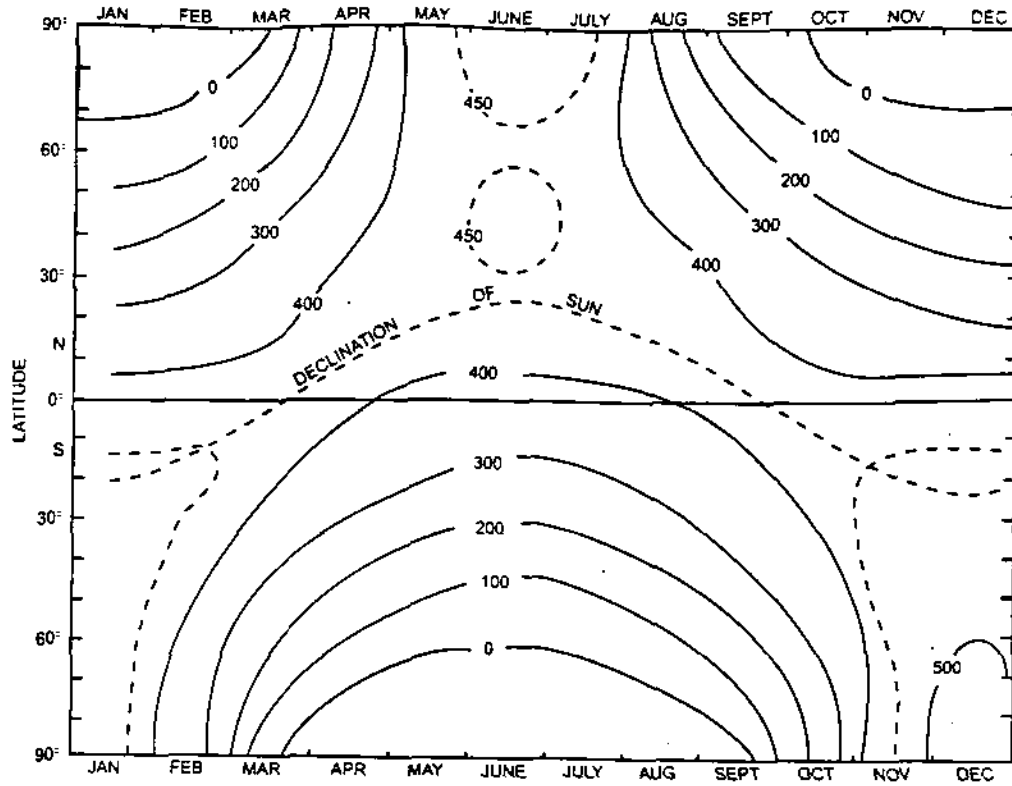

FIGURE 2.7 Distribution of solar radiation at top of atmosphere (in Watt hours per square meter). Apparent position of Sun overhead at noon (declination) is shown by dotted line.

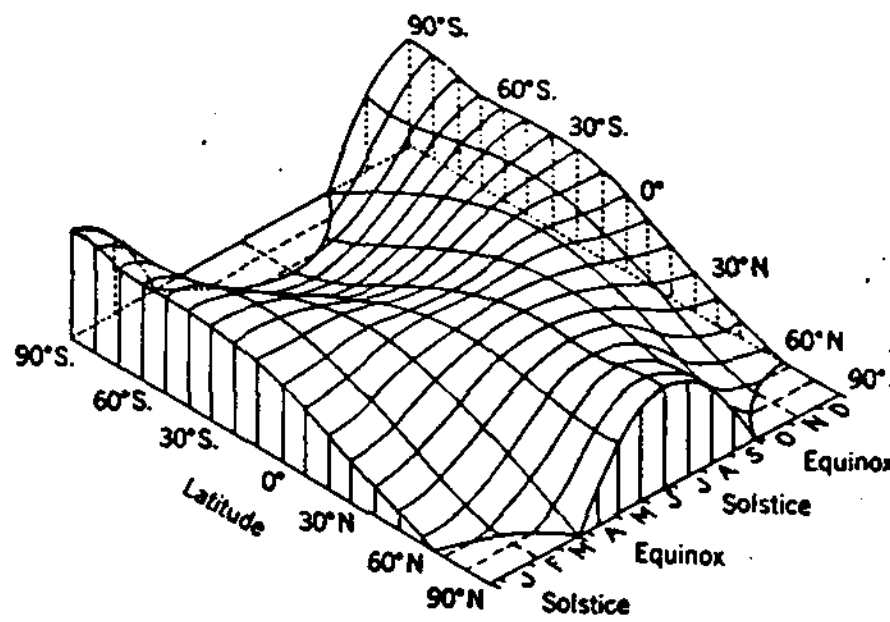

Figure 2.4 The variations of solar radiation with latitude and season for the whole globe, assuming no atmosphere. This assumption explains the abnormally high amounts of radiation received at the poles in summer, when daylight lasts for 24 hours each day.

Source: After W. M. Davis.

Appendix A1

Radiation geometry

1 BEAM RADIATION

(a) Sun–Earth geometry

Figure A1.1 illustrates the geometrical relations between the Earth and the solar beam radiation, and defines the following angles:

ϕ – the latitude of the location, the angle between the equatorial plane and the site of interest (point X in the figure), considered positive in the Northern and negative in the Southern Hemisphere.

δ – the *solar declination*, the angle between the Sun's rays and the equatorial plane.

Z – the *solar zenith angle*, the angle between the Sun's rays and the zenith direction. The zenith direction in the figure is the extension of the line connecting the centre of the Earth and the point X, i.e. directly overhead. The complementary angle $(90°-Z)$ is β, the *solar altitude* or elevation (not shown), and is the angle between the Sun and the local horizontal.

h – the *hour angle* is the angle through which the Earth must turn to bring the meridian of the site X directly under the Sun. It is a function of the time of day. It is related to, but distinct from, Ω.

Ω – the *solar azimuth angle*, which is the angle between the projections onto the horizontal plane of the site of both the Sun and the direction of true north. The azimuth angle is measured clockwise from north (0–360°); it is not illustrated in Figure A1.1, but see Figure A1.4.

Spherical trigonometry gives the following relationships between the angles:

$$\cos Z = \sin\phi \sin\delta + \cos\phi \cos\delta \cos h = \sin\beta \qquad \text{(A1.1)}$$

$$\cos\Omega = (\sin\delta \cos\phi - \cos\delta \sin\phi \cos h)/\sin Z;\ t < 12 \qquad \text{(A1.2)}$$

$$= 360° - (\sin\delta \cos\phi - \cos\delta \sin\phi \cos h)/\sin Z;\ t > 12$$

where t is *local apparent solar time*.

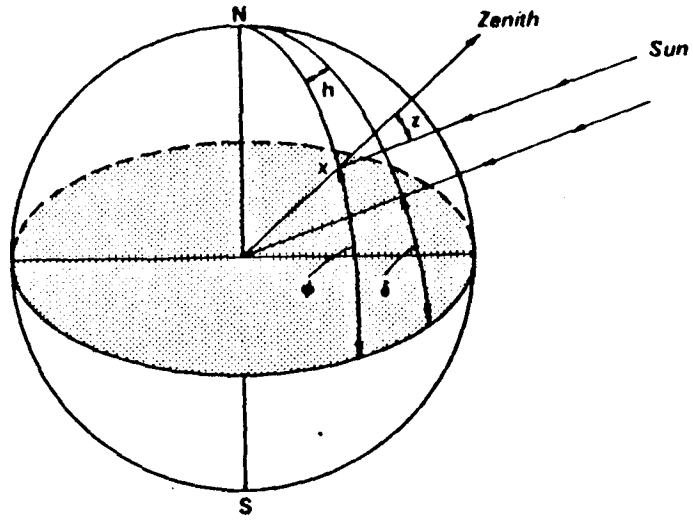

Figure A1.1 Geometrical relations between the Earth and the solar beam (S). The angles (see text) are defined with reference to the equatorial plane (shaded) and the point of interest (X).

The solar declination is dependent only upon the day of the year (see Table A1.1); to a first approximation it may be calculated from:

$$\delta = -23{\cdot}4\cos[360(t_j + 10)/365] \qquad \text{(A1.3)}$$

where t_j is the Julian date (number of the day) in the year. Accurate information is published in almanacs.

Since 1 hour is equivalent to 15° of Earth rotation the hour angle (h) is given by:

$$h = 15(12 - t) \qquad \text{(A1.4)}$$

where t is the local apparent solar time (using a 24-hour clock).

To calculate local apparent solar time: (i) add (subtract) 4 min to local standard time for each degree of longitude the site is east (west) of the standard meridian; this gives the *local mean solar time*. Now: (ii) algebraically add the *equation of time* correction (see Table A1.1) to (i) in order to get the local apparent solar time (see p. 401).

Using the cosine law of illumination (equation 1.9, p. 13) and equation A1.1 it is straightforward to calculate the solar radiation impinging at the top of the atmosphere at any location and time as $I_0 \cos Z$, where I_0 is the solar constant (p. 18).

It is also useful to note that the daylength t_d (number of hours with the Sun above the horizon) for an unobstructed horizontal site can be found

3. PRECESSION OF EQUINOX

THIS IS DETERMINED BY AXIAL TILT AND EARTH'S NON-SPHERICITY

A. CLIMATIC PRECESSION – RELATIVE TO a moving PERIHELION

e sin υ

Period 21.7 Ka

MAXIMUM EFFECT OF e sin υ
- LOW LATS
OPPOSITE SIGN BETWEEN HEMISPHERES

B. ASTRONOMICAL PRECESSION – RELATIVE TO a fixed PERIHELION

Period 25.7 Ka

THESE 2 MEASURES GO IN OPPOSITE DIRECTIONS

LARGE e EXAGGERATES THE PRECESSIONAL EFFECT

NET ENERGY VARIATIONS ABOUT ±30 W m^{-2} AT SOME LATITUDES (i.s. 2% of S_0)

ORBITAL FORCINGS AND CHARACTERISTICS

ELEMENT	INDEX RANGE	PRESENT VALUE	AVERAGE PERIODICITY
OBLIQUITY OF ECLIPTIC (ε) (TILT OF AXIS OF ROTATION)	22^0 - 24.5^0	23.4^0	41 k a
Effects equal in both hemispheres, effect intensifies polewards (for caloric seasons)			
Low ε / *High* ε			
Weak seasonality, steep poleward radiation gradient / Strong seasonality, more summer radiation at poles, weaker radiation gradient			
PRECESSION OF EQUINOX (ω) (WOBBLE OF AXIS OF ROTATION)	0.05 to -0.05	0.0164	19, 23 k a
Changing Earth-Sun distance alters seasonal cycle structure; complex effect, modulated by eccentricity of orbit.			
ECCENTRICITY OF ORBIT (e))	0.005 to 0.0607	0.0167	410, 95 k a
Gives 0.02% variation in incoming radiation; modifies amplitude of precession cycle changing seasonal duration and intensity; effects opposite in each hemisphere; greatest in low latitudes.			

A. D. Vernekar, Variations in the insolation caused by changes in orbital elements of the earth, THE SOLAR OUTPUT AND ITS VARIATION, Oran R. White, ed., p. 122

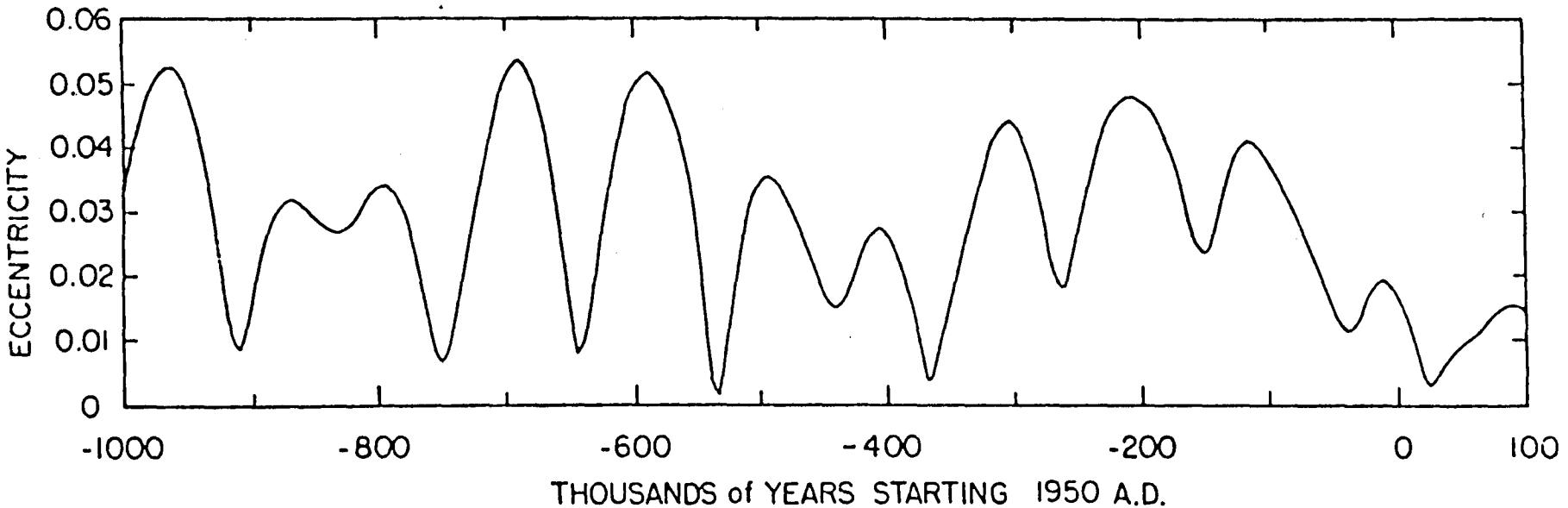

Fig. 1. The variation of eccentricity of the earth's orbit as a function of time for the period from 1,000,000 before 1950 A.D. to 100,000 years in the future.

A. D. Vernekar, Variations in the insolation caused by changes in orbital elements of the earth, THE SOLAR OUTPUT AND ITS VARIATION, Oran R. White, ed., p. 126

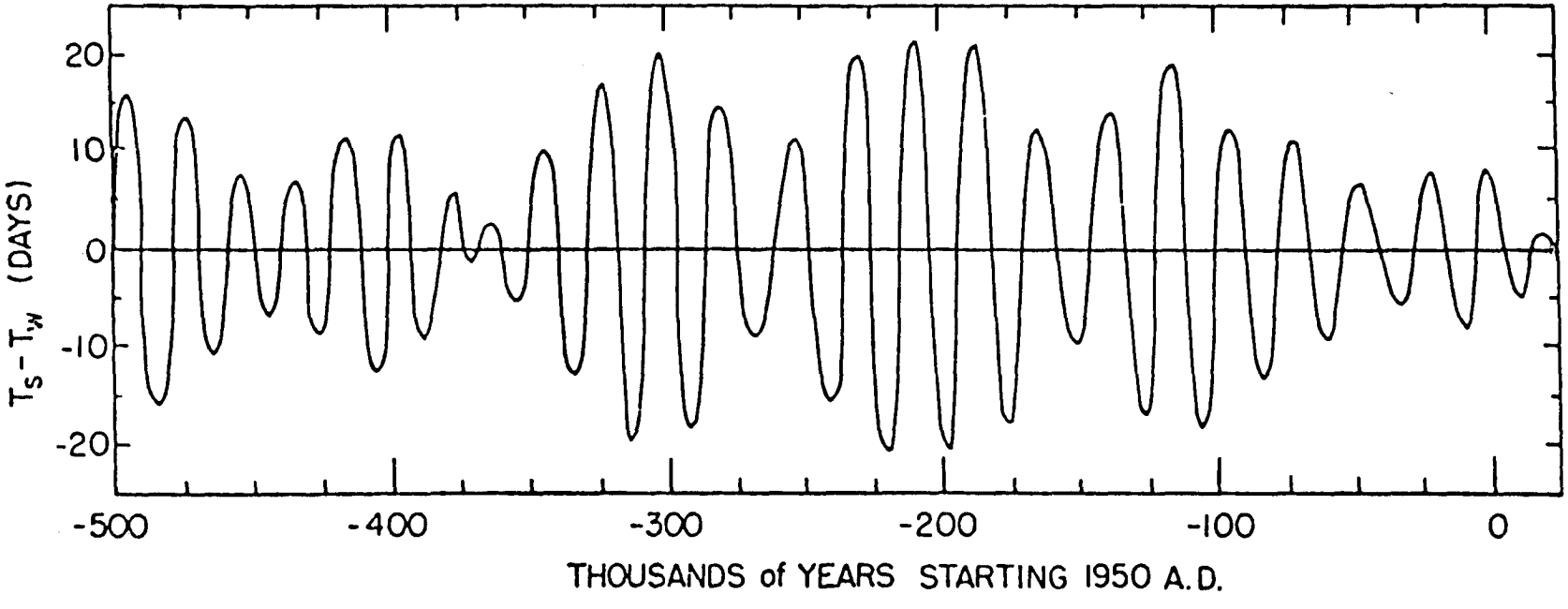

Fig. 4. The variation of difference between the duration of astronomical summer half, T_S, and that for the winter half, T_W, as a function of time for the period from 500,000 years before 1950 A.D. to 25,000 years in the future.

A. D. Vernekar, Variations in the insolation caused by changes in orbital elements of the earth, THE SOLAR OUTPUT AND ITS VARIATION, Oran R. White, ed., p. 122

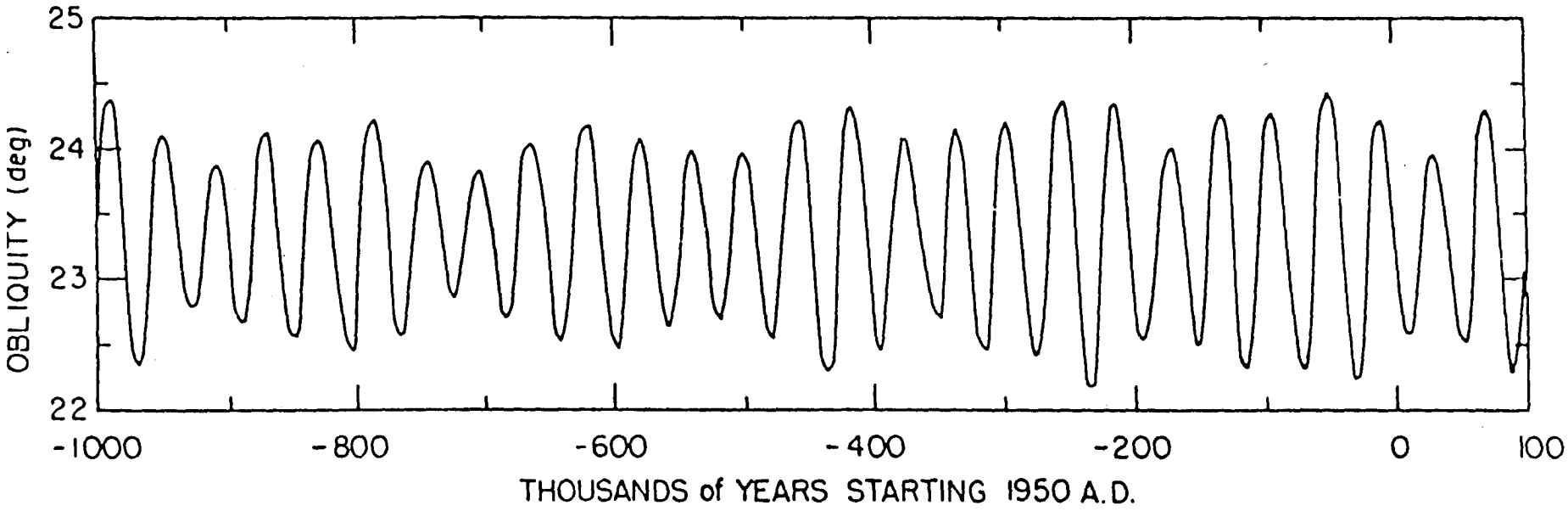

Fig. 2. The variation of earth's obliquity as a function of time for the period from 1,000,000 years before 1950 A.D. to 100,000 years in the future.

A. D. Vernekar, Variations in the insolation caused by changes in orbital elements of the earth, THE SOLAR OUTPUT AND ITS VARIATION, Oran R. White, Ed., p. 123

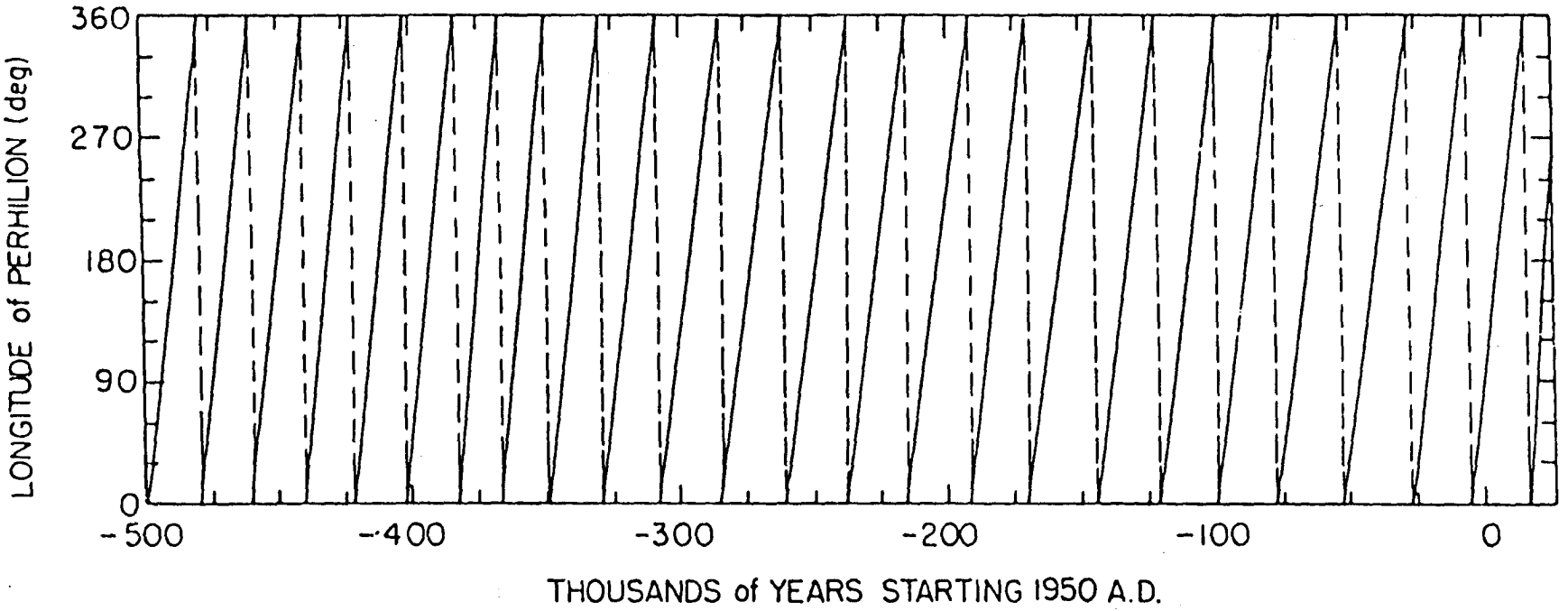

Fig. 3. The variation of the longitude of perihelion from moving equinox as a function of time for the period from 500,000 years before 1950 A.D. to 25,000 years in the future.

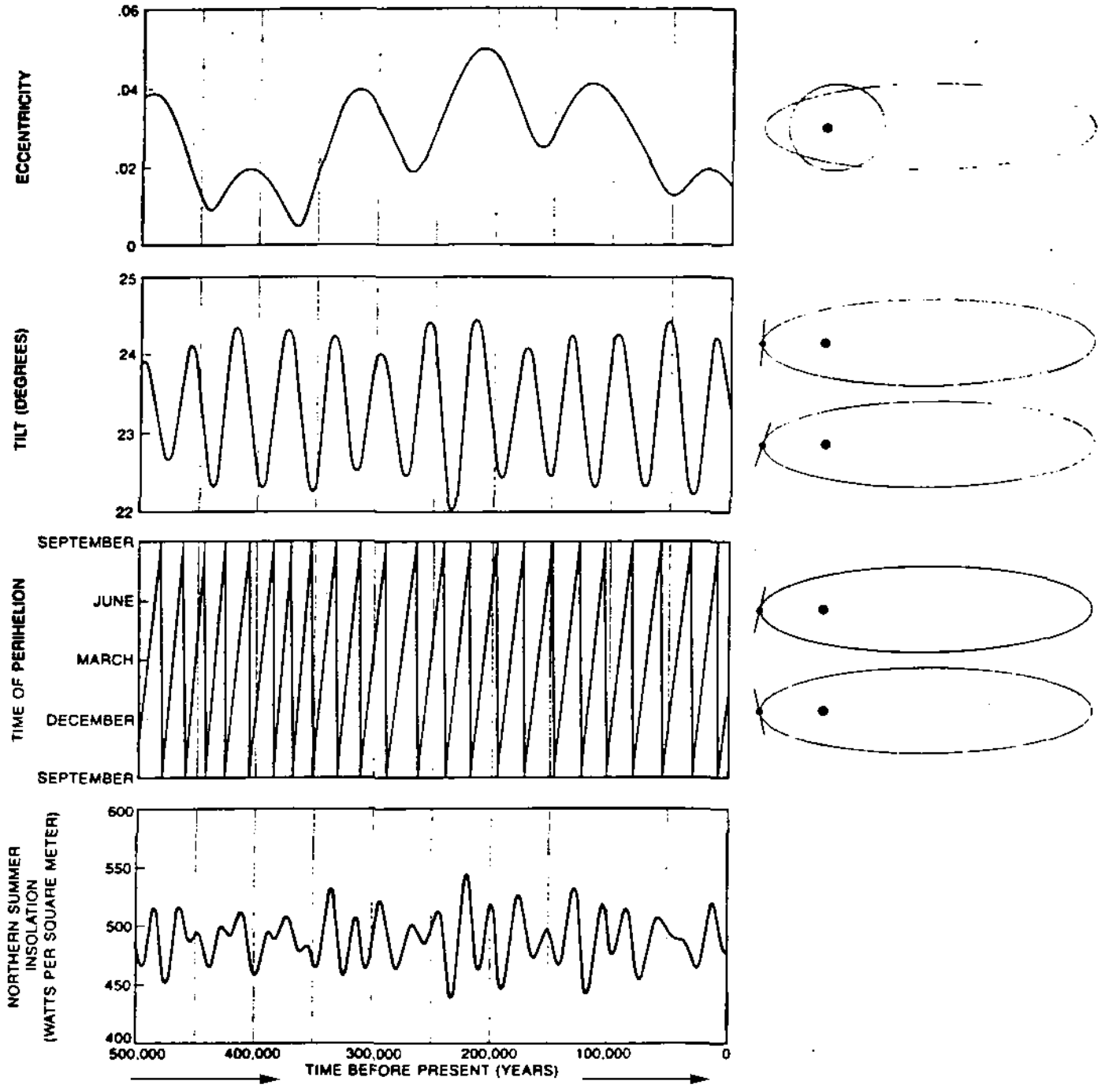

MILANKOVITCH THEORY, formulated by the Yugoslav astronomer Milutin Milankovitch, attributes the onset of ice ages to variations in three parameters of the earth's orbit. The eccentricity is the degree to which the orbit departs from a perfect circle. The tilt angle is the angle between the earth's axis and a direction perpendicular to the plane of its orbit. The time of perihelion determines the direction in which the axis points when the earth makes its closest approach to the sun. Each of the parameters changes slowly under the influence of the gravitational attraction of the moon and of the other planets. Changes in the orbital parameters lead to changes in the amount of sunlight received by the earth; there is little change in the annual global insolation but there are relatively large changes in high-latitude summertime insolation. The variations in eccentricity, tilt and the time of perihelion were calculated by a method developed by André Berger. Times of maximum eccentricity are separated by periods of roughly 100,000 years, although the eccentricity has a second period of roughly 400,000 years. The cycles of tilt and time of perihelion have periods of approximately 40,000 and 20,000 years. The time of perihelion is also not a simple sine curve; it has two cycles of 19,000 and 23,000 years. Variation in the amount of sunlight received is shown for the zone between 60 and 70 degrees north latitude in July. Insolation was calculated with a computer program written by Tamara S. Ledley of the Massachusetts Institute of Technology and Stanley L. Thompson of the National Center for Atmospheric Research.

Covey, C., 1984: The Earth's orbit and the ice ages, Scientific American, 250, 58-66.

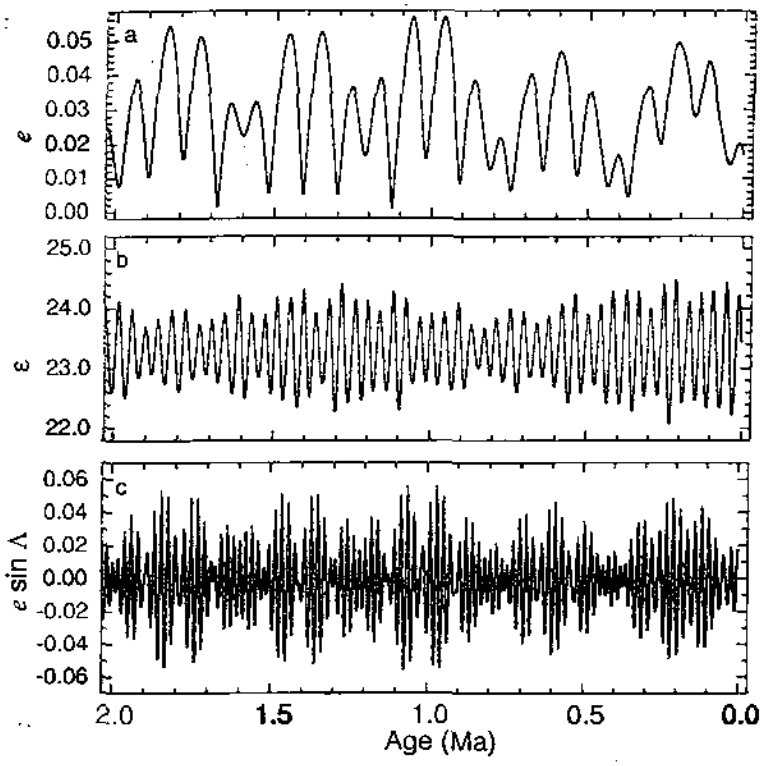

Figure 1-7 Secular variation of the orbital parameters for the past 2 My according to the expansion of the secular variations of the orbital parameters given by Berger and Loutre (1991). (a) The secular behavior of the eccentricity forcing of the solar constant, e. (b) The secular behavior of the obliquity of the Earth's orbit, ε, in degrees. (c) As above but for the precessional index $e \sin \Lambda$. Notice how the spectral characteristics do not change appreciably between the early and late Pleistocene, but, the paleoclimatic record does.

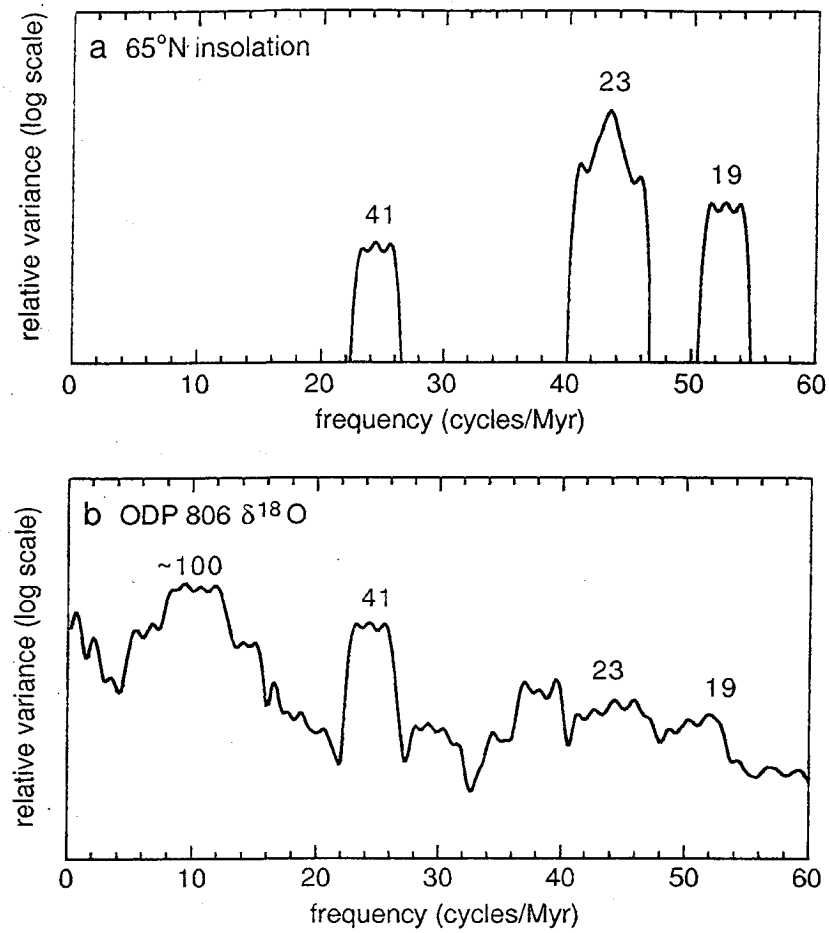

Figure 1-10 Comparison of (a) the spectrum of incoming summer radiation at 65°N due to the Earth-orbital changes shown in Fig. 1-9a with (b) the spectrum of ice mass variations shown in Fig. 1-9b over the past 1 My. The numbers at the top of the spectral peaks are the approximate periods in 10^4-year units (ky).

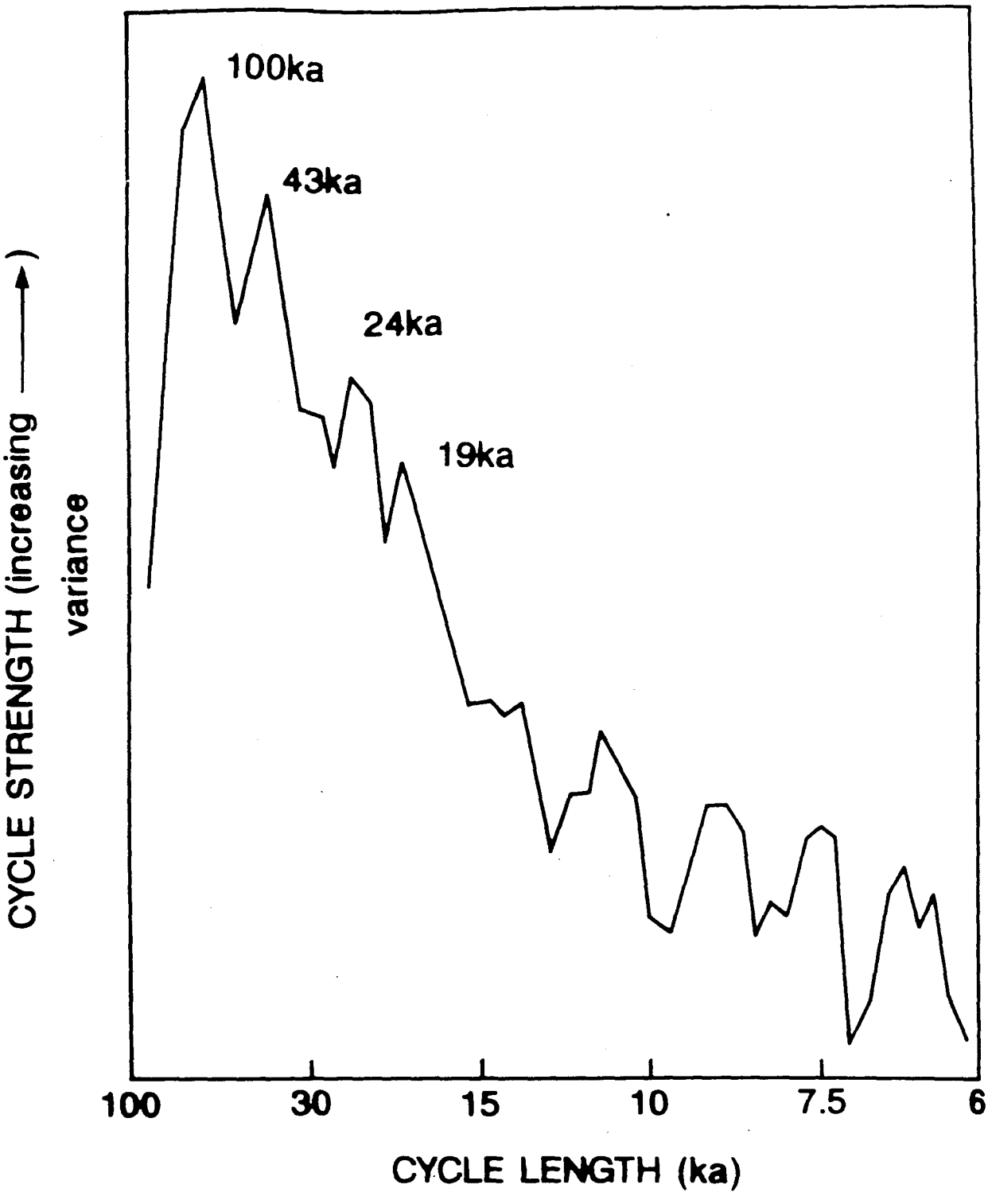

Figure 2.5 Spectral analysis of a 500 ka record from two Indian Ocean cores. Peaks of high relative variance are labelled. (Data from Hays *et al.*, 1976; figure from Imbrie and Imbrie, 1979.)

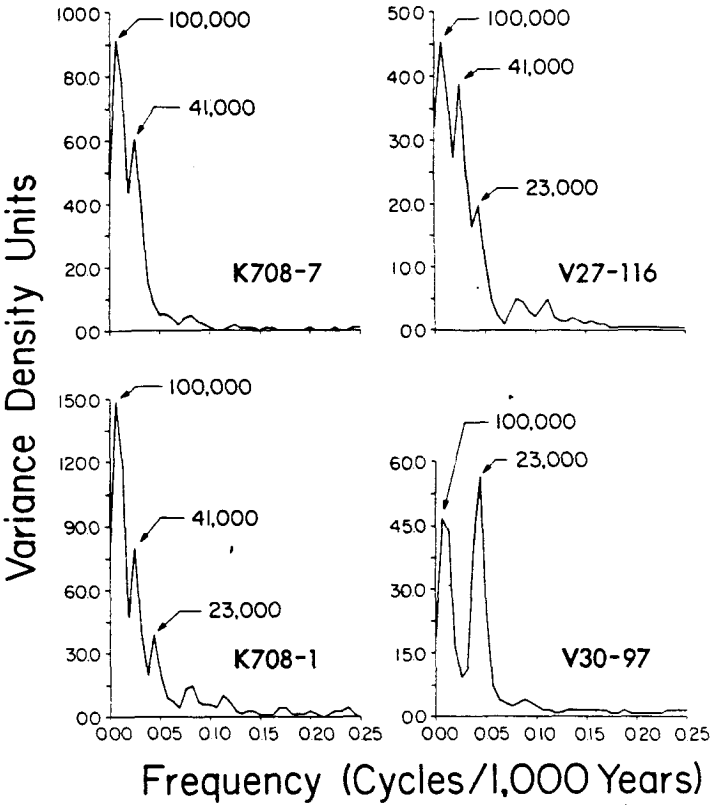

Figure 20. Variance density plots of estimated August sea-surface temperature in four of the seven cores shown in figure 19. The 100,000-year rhythm is strong in all regions; the 41,000-year power is strongest in the three northern cores but yields to 23,000-year power in mid-latitude core V30-97 (from ref. 89.

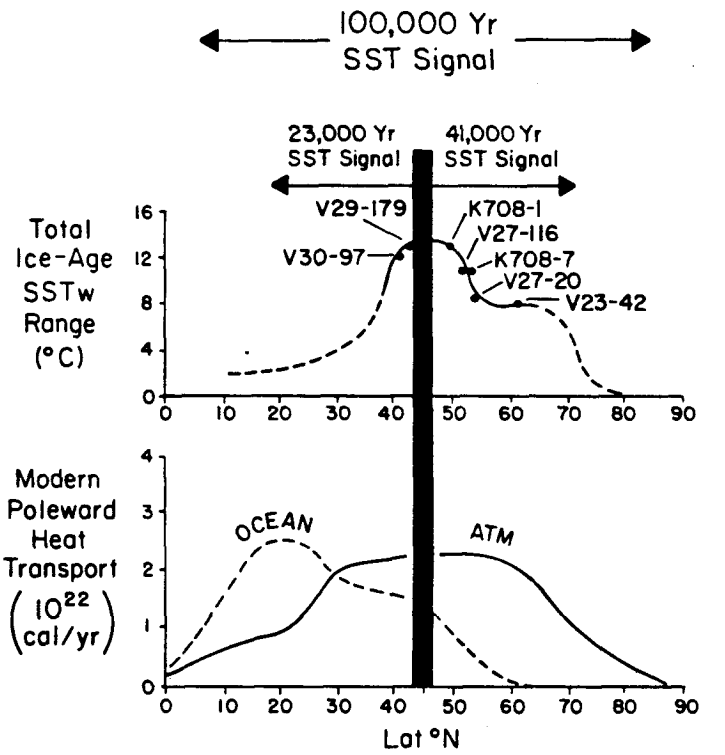

Figure 22. Summary of late Quaternary North Atlantic SST response. Top: Amplitude of glacial/interglacial SST change, with regions of spectral dominance superimposed. Cores are those in figure 19. Bar is boundary of 41,000-year and 23,000-year responses. Bottom: Estimated amount of energy carried poleward by ocean and atmosphere in Northern Hemisphere (from ref. 89).

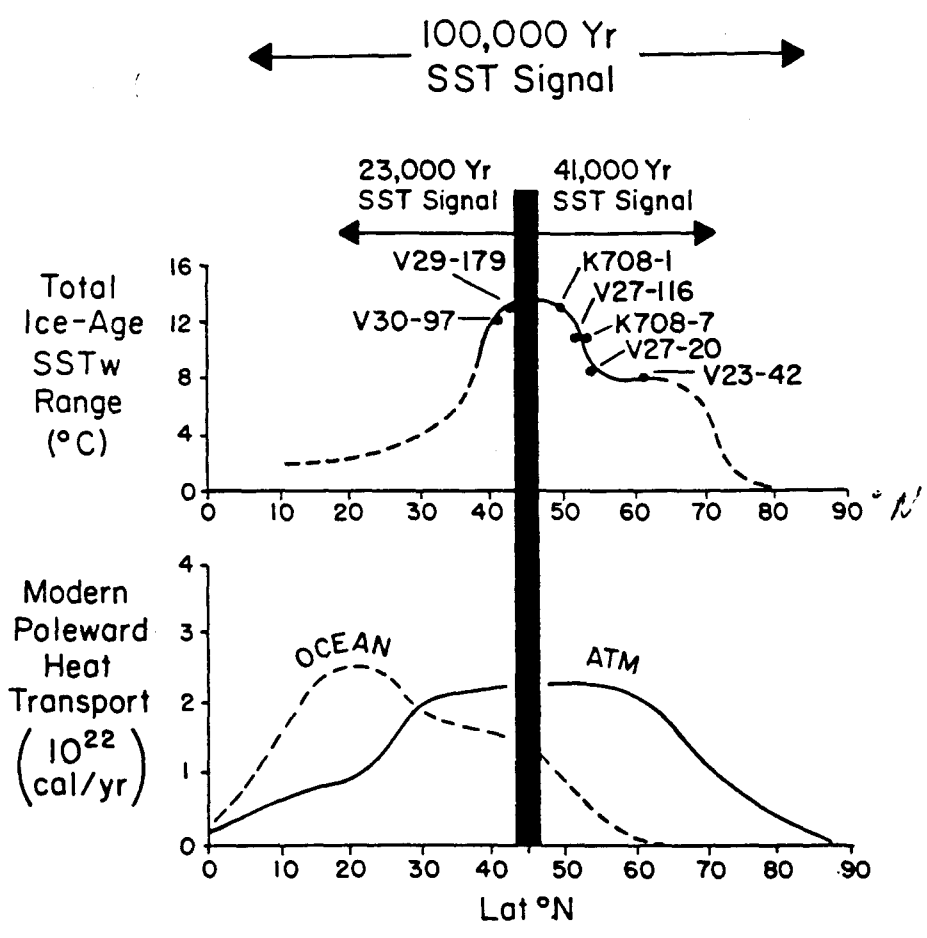

Figure 2 (top) Glacial/interglacial amplitude of SST change and geographic partitioning of frequency response (from 27); (bottom) Estimate of modern poleward transport of heat by the Northern Hemisphere oceans and atmosphere (from 28).

History of Orbital Theory

1842	J. Adhemal	Role of axial tilt variations
1875	J. Croll	Proposed glaciations = cold winters (modern view is converse) recognized role of snow albedo
1920's	M. Milankovitch	Calculated periodicities to 600 Ka and used them to "date" Gunz, Mindel, Riss Wurm
1972	A.D. Vernekar (Met. Monogr.)	
1976	J. Hays, J. Imbrie, N. Shackleton (1976) Pacemaker of the ice ages	
1977	A. Berger Refines Calculations	

Conditions for Glaciation (NOTE: latitudinal dependencies)

- Small seasonal difference (in higher latitudes) i.e. small ε
- Summer at aphelion (cooler summer)
- Large e (amplifies cool summer; affects low latitudes)

Magnitude of Forcing

- Direct effects (radiation) ~0.5 K (J. Hansen et. al. 1984) therefore, feedbacks essential
- Climate responses (glacier build up/decay) will lag by 5-10 Ka
- Hemispheric Glacials~Synchronous! Land/sea contrasts, deep water circulation

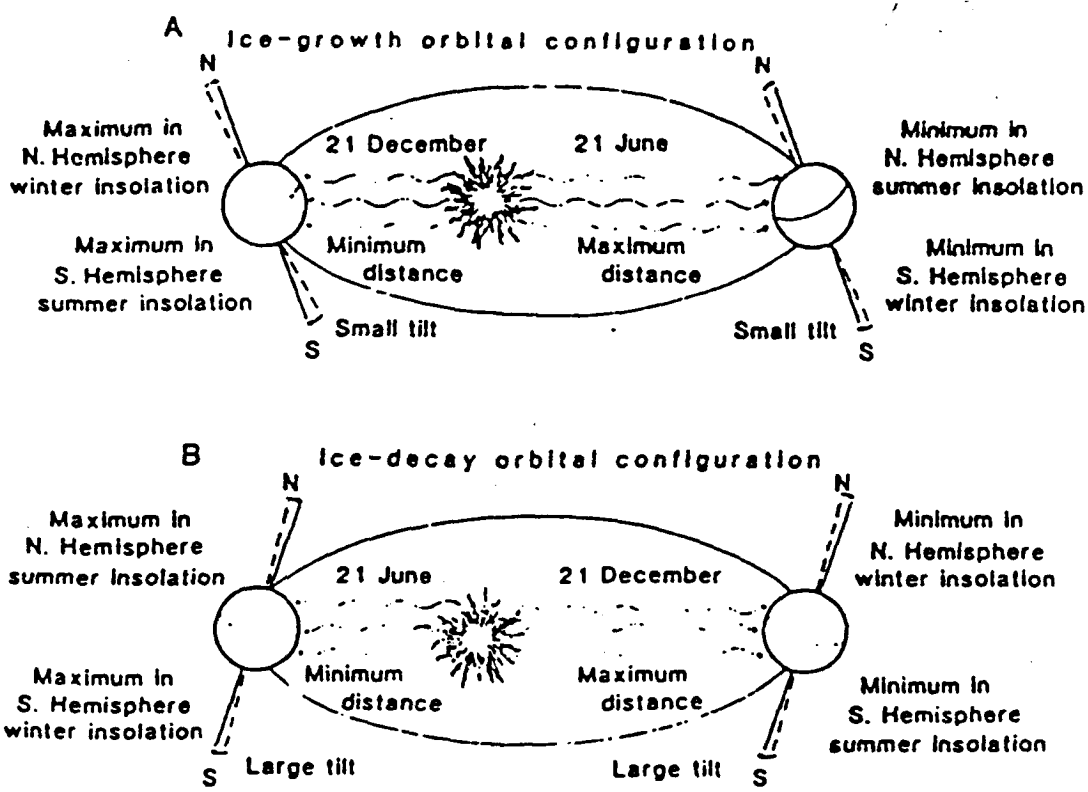

Fig. 1. (A) Orbital configuration of the earth and sun during periods of rapid ice growth based on Milankovitch (*1*). Critical summer season of minimal insolation and ice melting in the Northern Hemisphere is related to low tilt and 21 June aphelion precession position (distant pass in the slightly eccentric orbit). (B) Orbital configuration during ice disintegration, as suggested by *Emiliani and Geiss [in (22)] and Broecker (41)*. *Maximum tilt and perihelion (close-pass)* 21 June precessional position favor high summer insolation and rapid ice disintegration in the Northern Hemisphere.

RUDDIMAN McINTYRE (Science 1981 v. 212 p. 618)

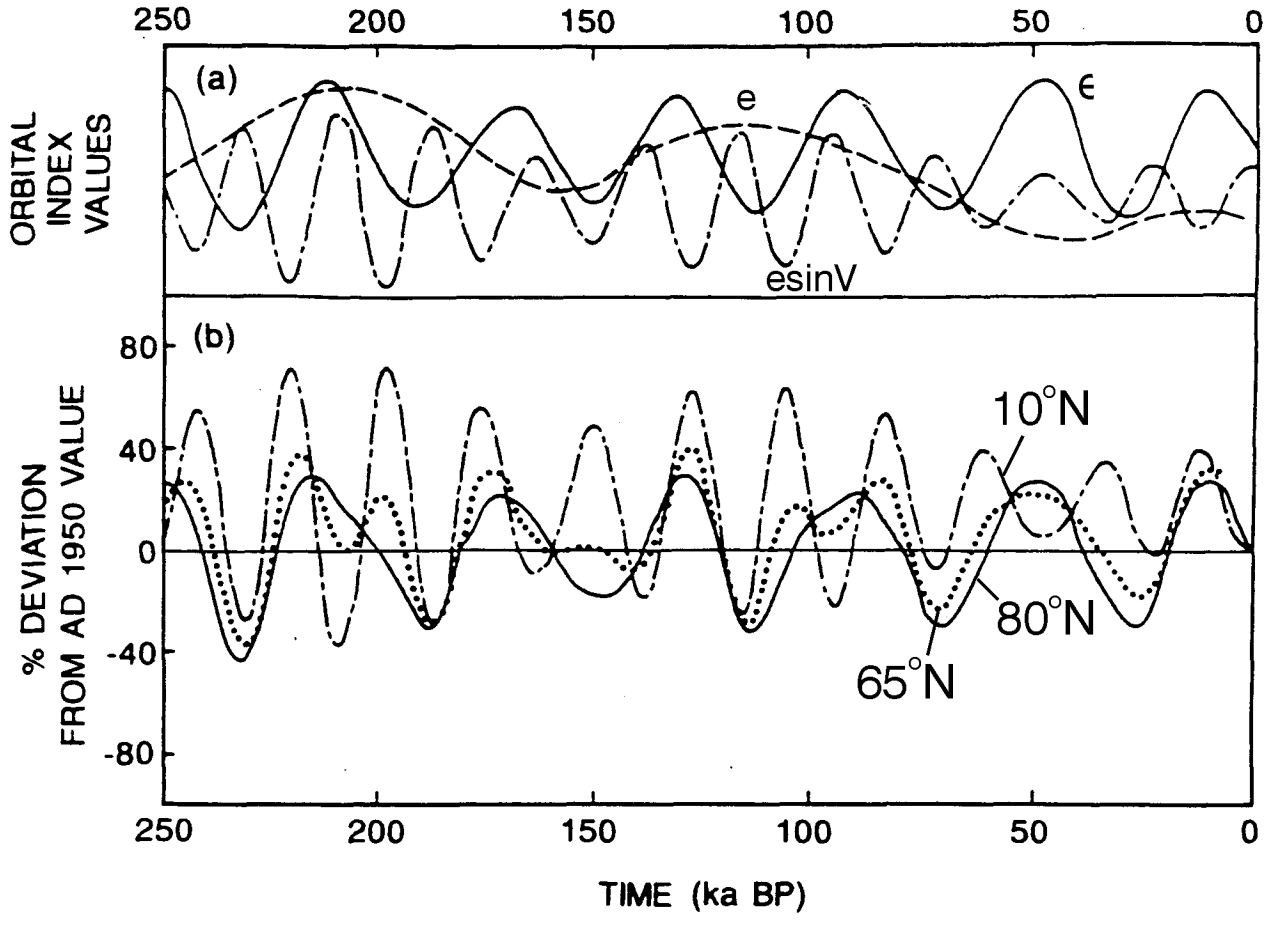

Figure 2.3 Orbital changes and solar insolation curves. (a) Variations of eccentricity (- - -), obliquity (——), and precession (– - – -), over the last 250 ka. (b) Northern Hemisphere summer solar radiation at 80°N (—), 65°N (·····), and 10°N (– - – -) expressed as percentage departures from 1950 values. (After Berger, 1978a.)

A. D. Vernekar, Variations in the insolation caused by changes in orbital elements of the earth, THE SOLAR OUTPUT AND ITS VARIATION, Oran R. White, Ed., p. 128

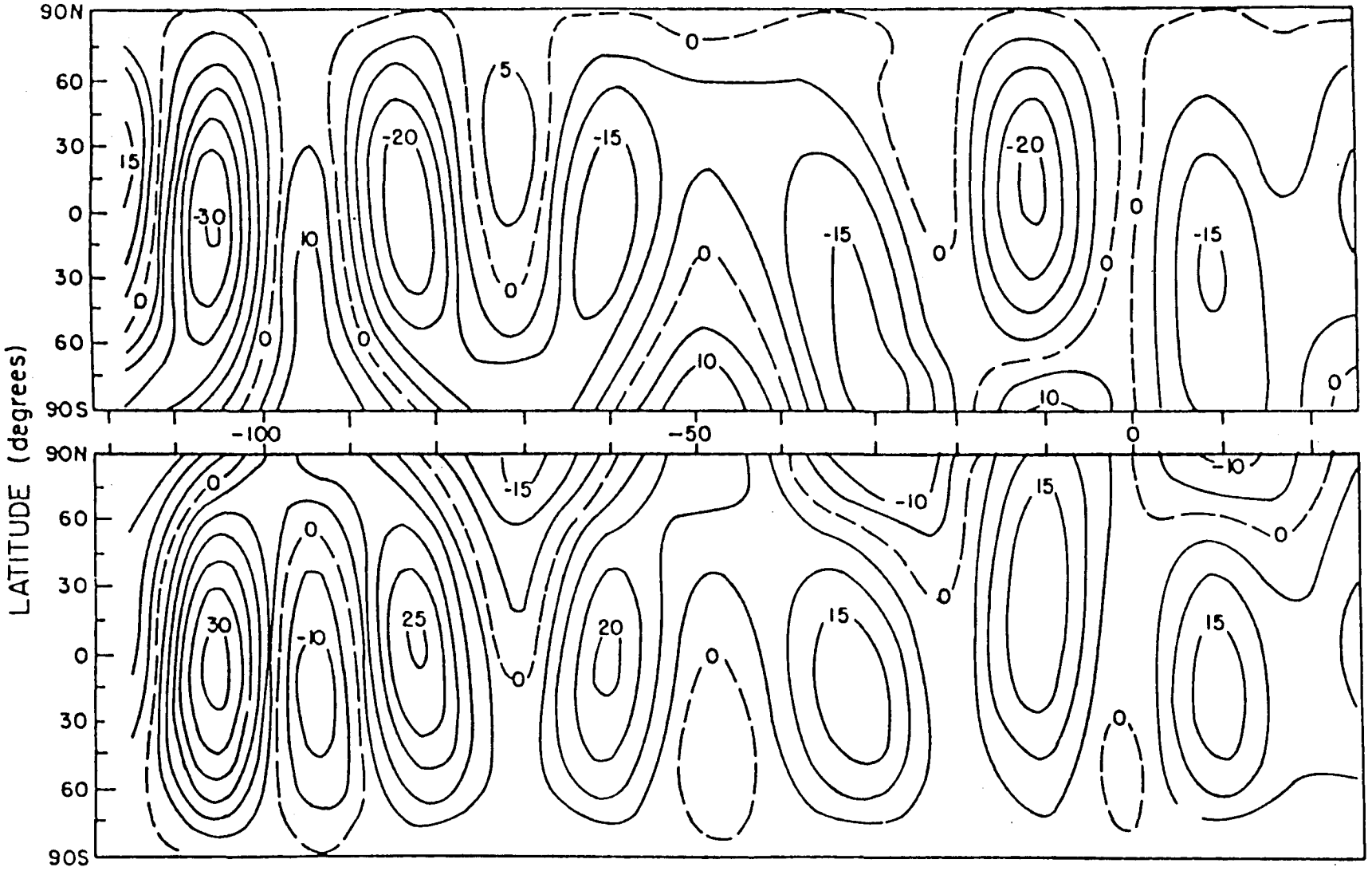

Fig. 5. The variation in ΔQ (deviation of the mean solar insolation from its present value) as a function of latitude and time in the units of Wm^{-2}. The upper half of the figure shows the variations for the northern caloric winter and southern caloric summer. The lower half shows the variations for the northern caloric summer and southern caloric winter. The abscissa shows the time (numbers between the two halves) in thousands of years. The variations shown in the figure are for the period from 115,000 years before 1950 A.D. to 25,000 years in the future.

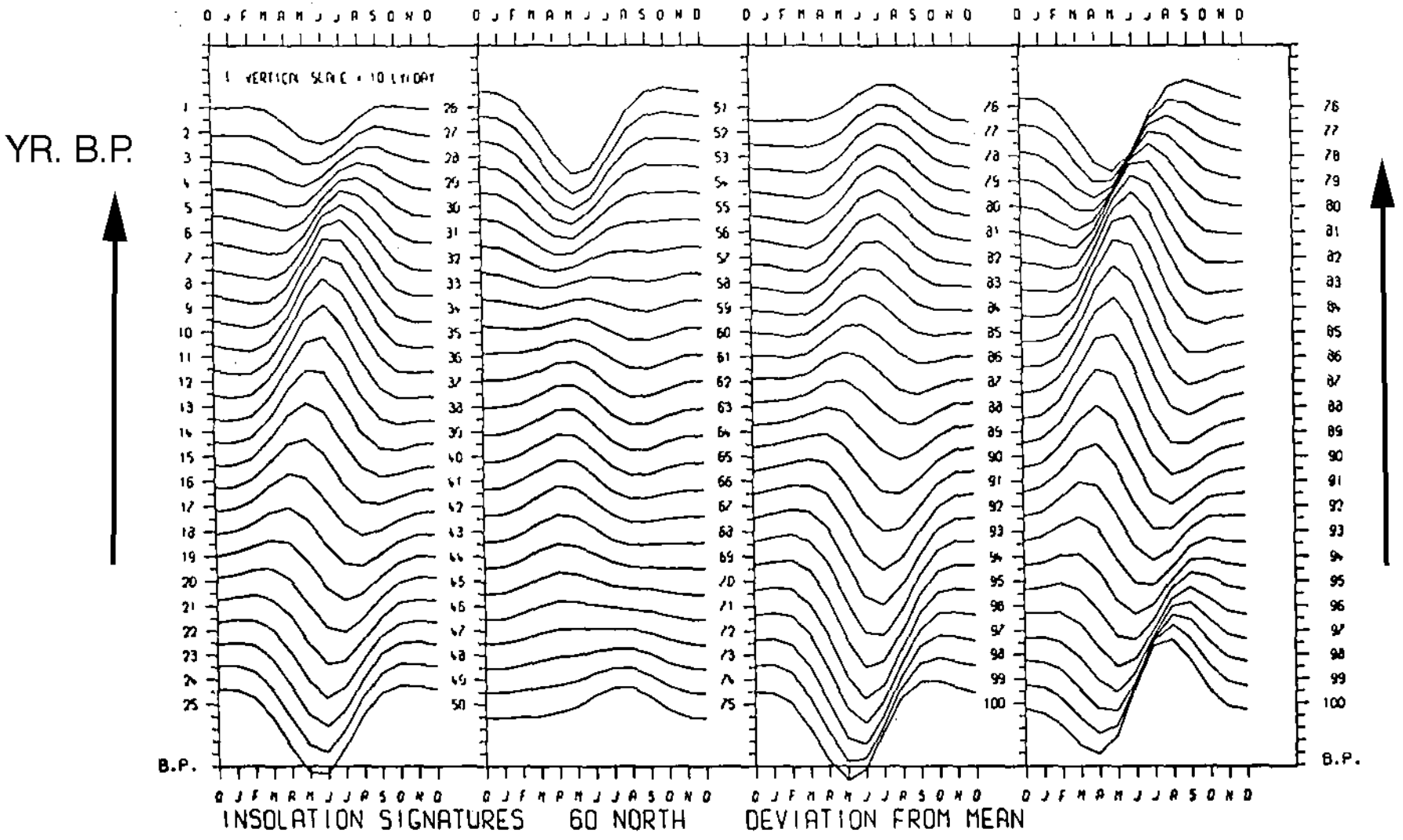
YR. B.P.
1 VERTICAL SCALE = 10 LY/DAY
B.P.
INSOLATION SIGNATURES 60 NORTH DEVIATION FROM MEAN
10 LY ~ 5 Wm-2

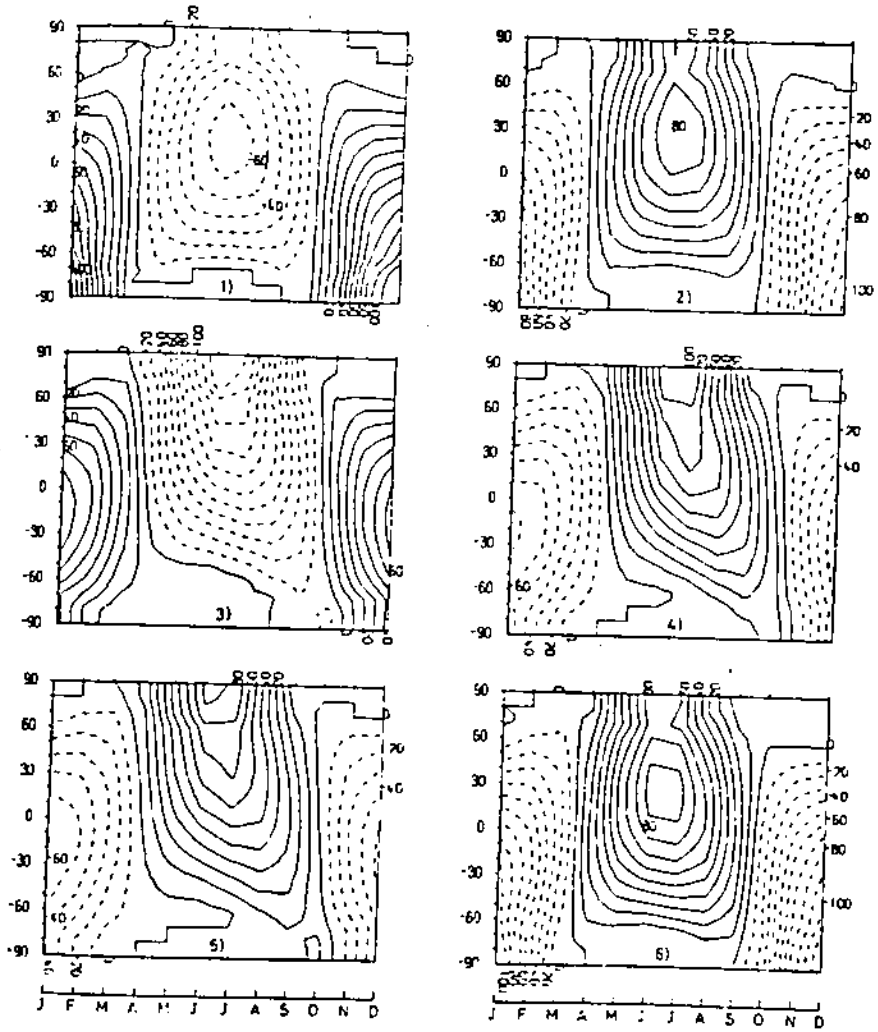

Figure 2 Latitudinal and month-to-month variations of the deviations of midmonth insolation from the mean state. These patterns are reproduced for 6 selected dates of the last 200 000 years. Isolines are drawn every 10 cal cm^{-2} d^{-1} and numbered every 20 cal cm^{-2} d^{-1}. Full lines are for positive deviations (insolation larger than today) and dashed lines characterize the insolation below their actual values. 1) 94 000 YBP, 2) 105 000 YBP, 3) 115 000 YBP, 4) 125 000 YBP, 5) 174 000 YBP, 6) 197 000 YBP. (from berger, 1979, (22))

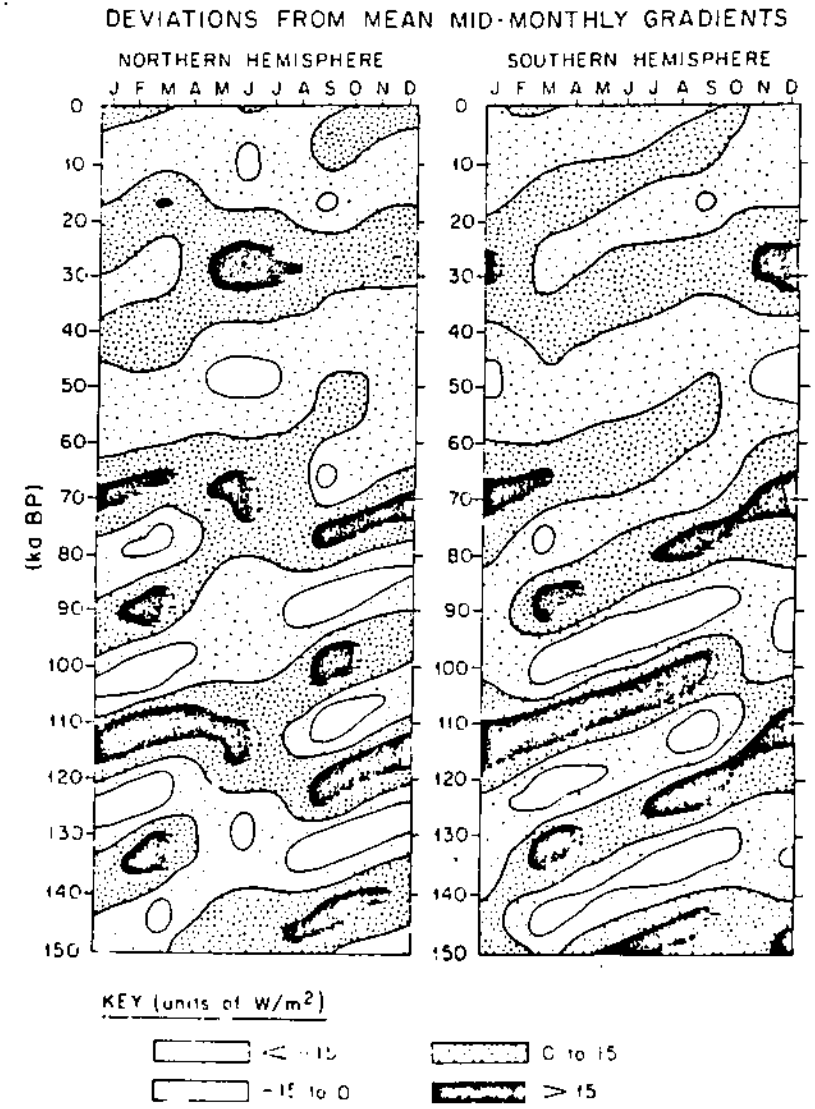

Figure 1 Deviations from monthly 150 kyr mean 30-90° insolation gradients for the Northern (left) and Southern (right) Hemipheres.

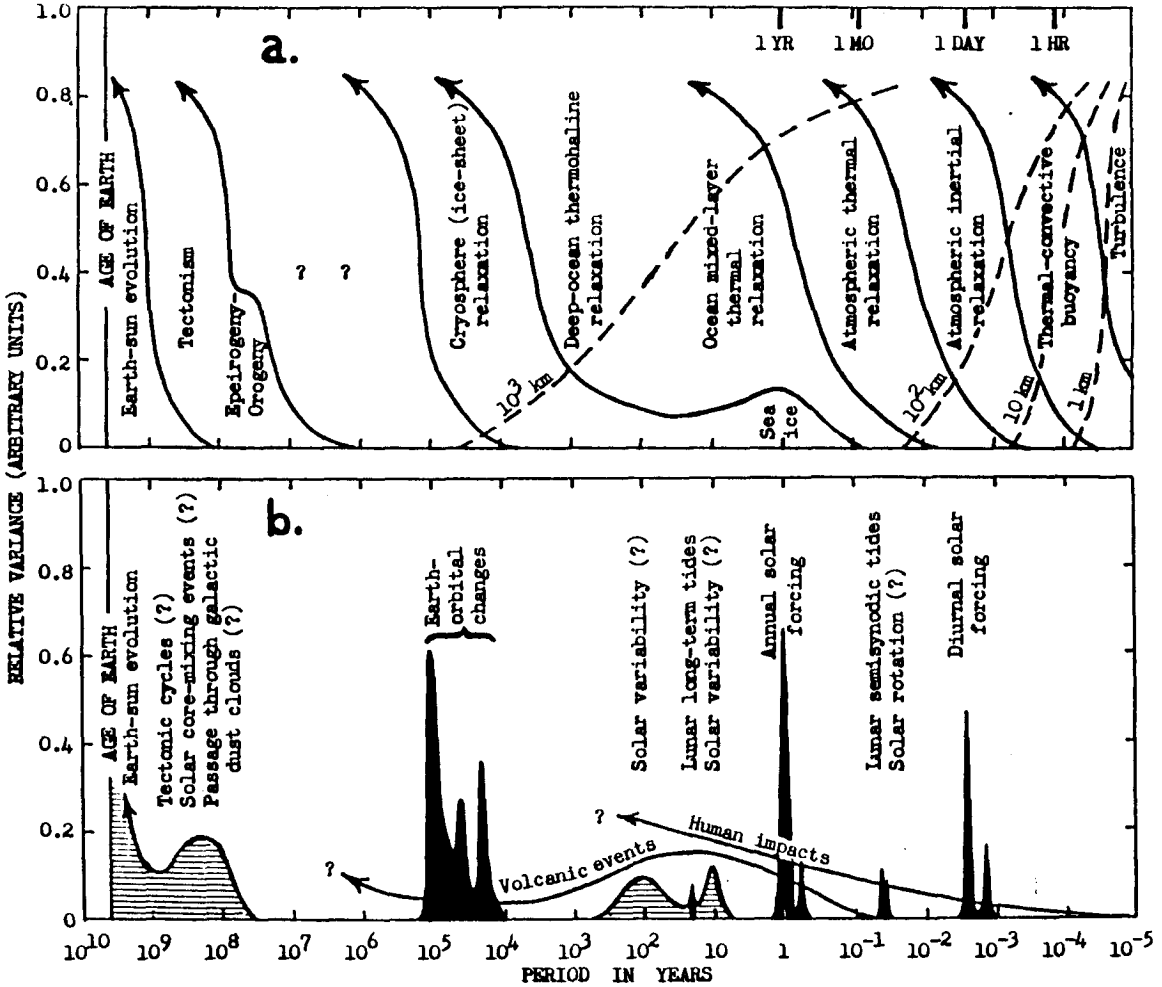

FIGURE 3

INTERNAL STOCHASTIC PROCESSES

---SPACIAL SCALE

EXTERNAL FORCINGS

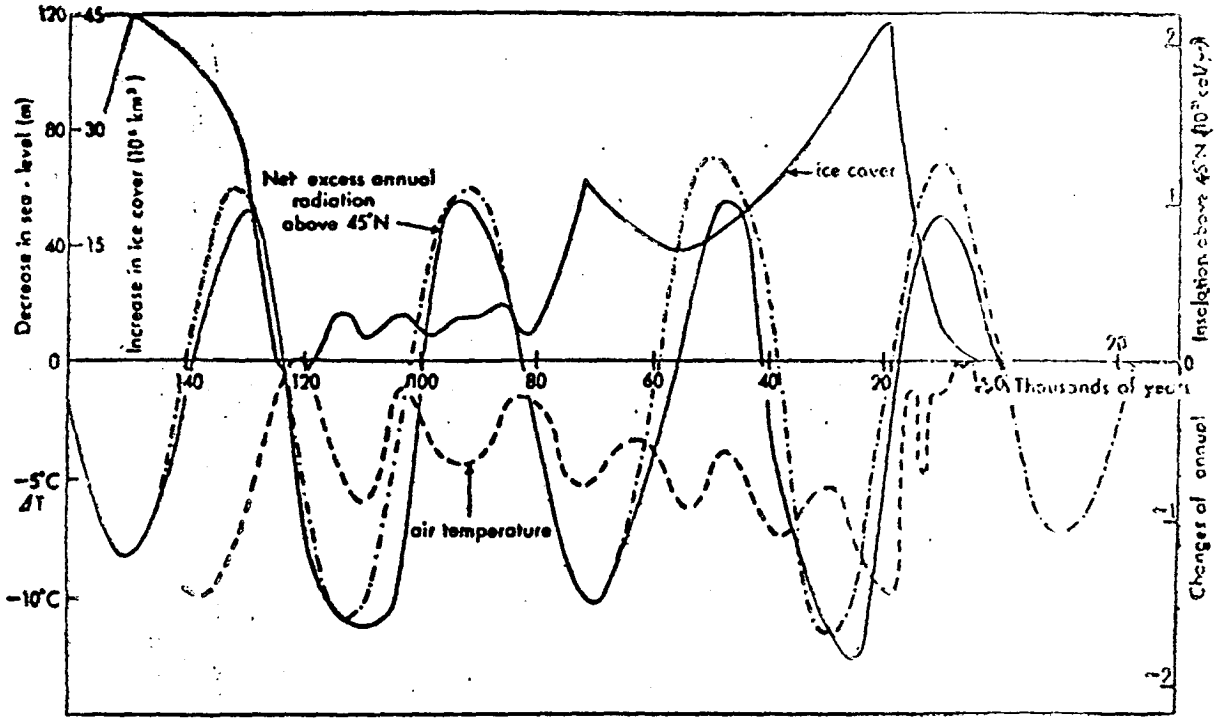

Figure 5 Changes in global ice cover, northern hemisphere air temperatures, and total insolation north of 45°N over the last 150 000 years. Total insolation plotted twice after Milankovitch and Vernekar. *After Mason (1976)*

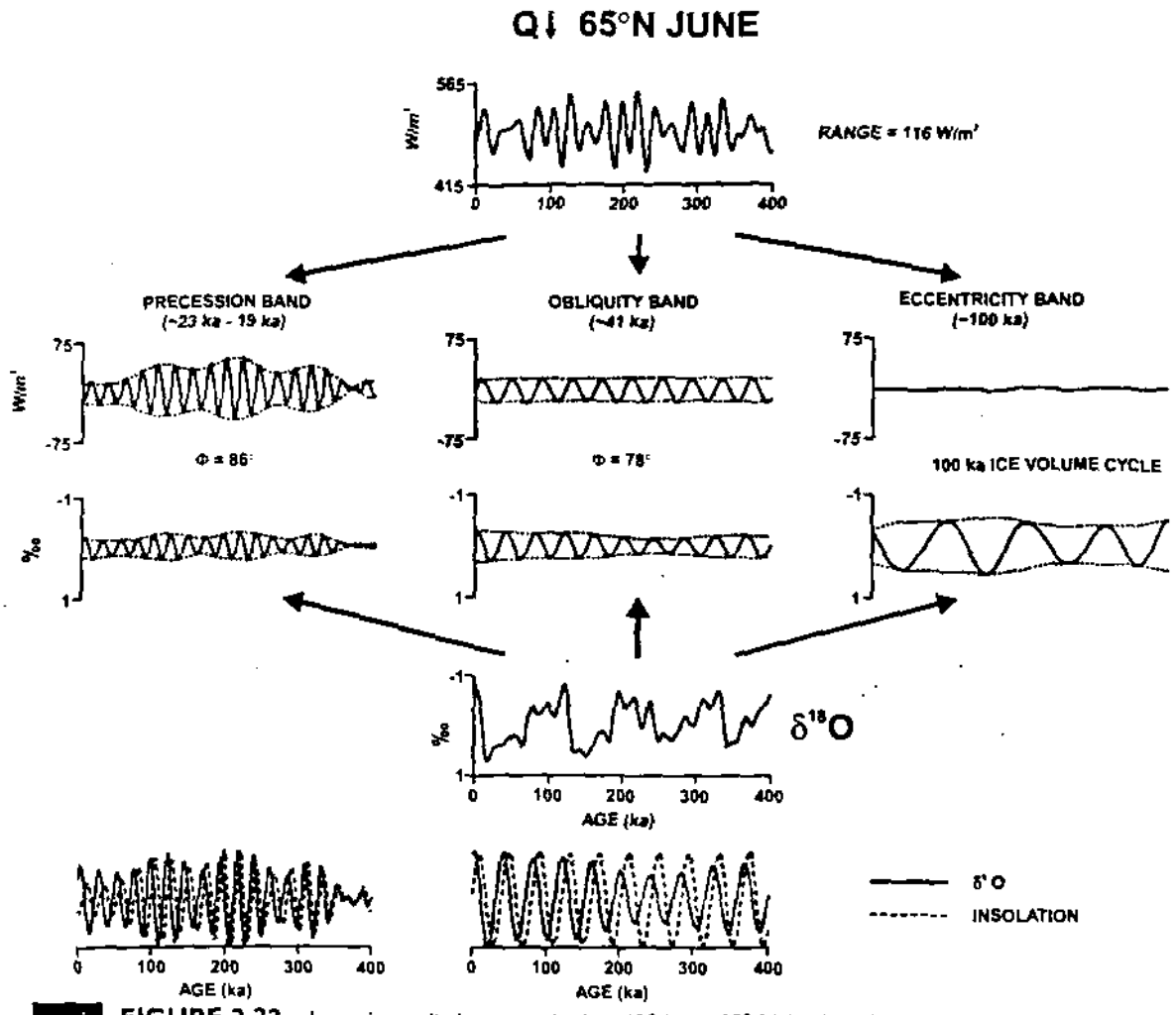

FIGURE 2.22 Incoming radiation over the last 400 ka at 65° N, broken down (bandpass filtered) into its principal orbital components (top) compared to the record of continental ice volume (recorded by $\delta^{18}O$ in marine sediments) and its principal components at the same frequencies (below). The lower panel shows the normalized precessional and obliquity bands in insolation and $\delta^{18}O$ superimposed to show the strong coherence between the radiation forcing and the continental ice volume response. The strong direct relationship between insolation changes related to obliquity and precession contrast strongly with the apparent lack of correspondence between the eccentricity forcing and the climate system response (from Imbrie et al., 1993a).

...ed (Raymo, 1998). For

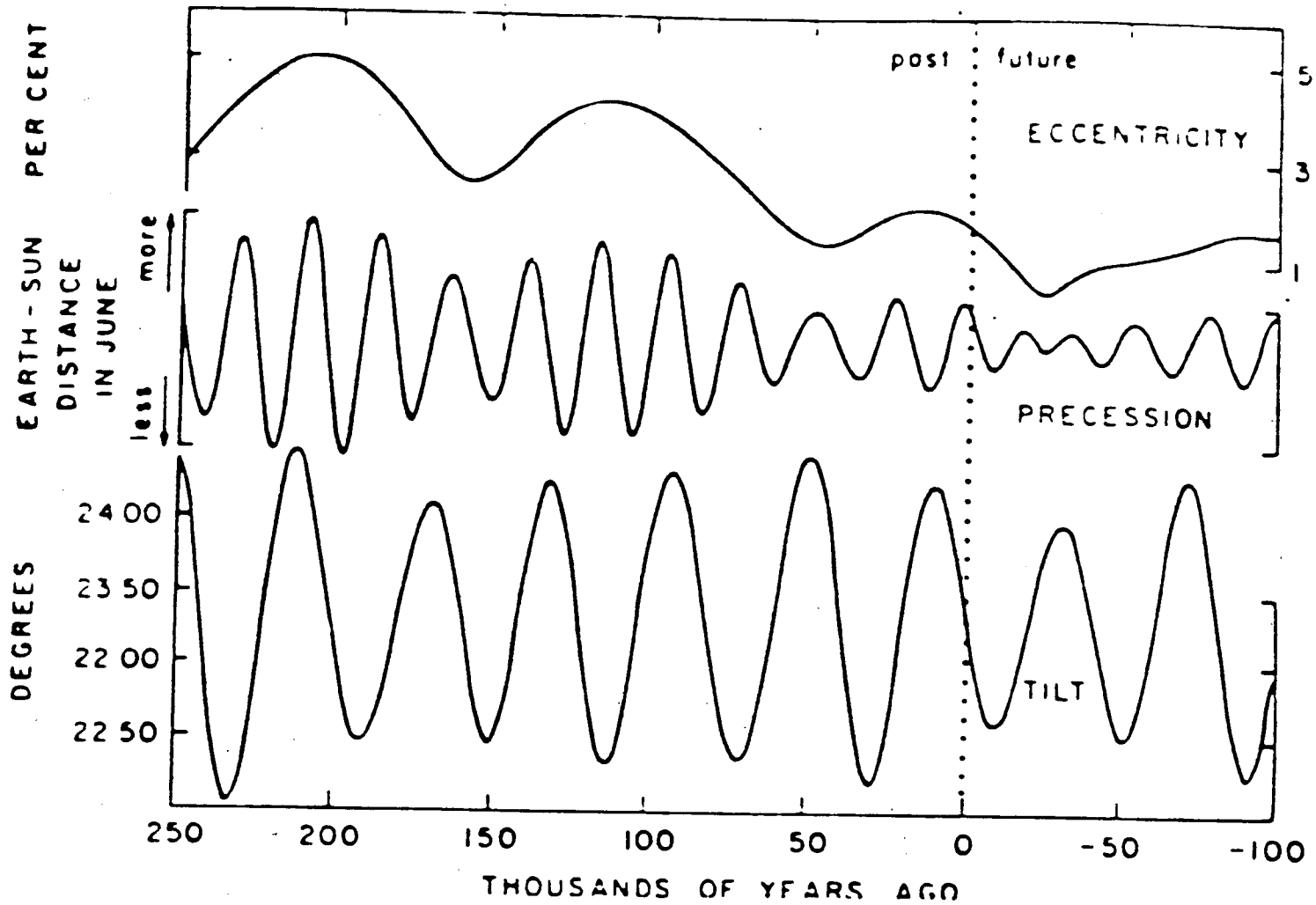
PER CENT
post
future
5
ECCENTRICITY
3
1
EARTH-SUN DISTANCE IN JUNE
more
less
PRECESSION
DEGREES
24 00
23 50
22 00
22 50
TILT
250
200
150
100
50
0
-50
-100
THOUSANDS OF YEARS AGO
Future

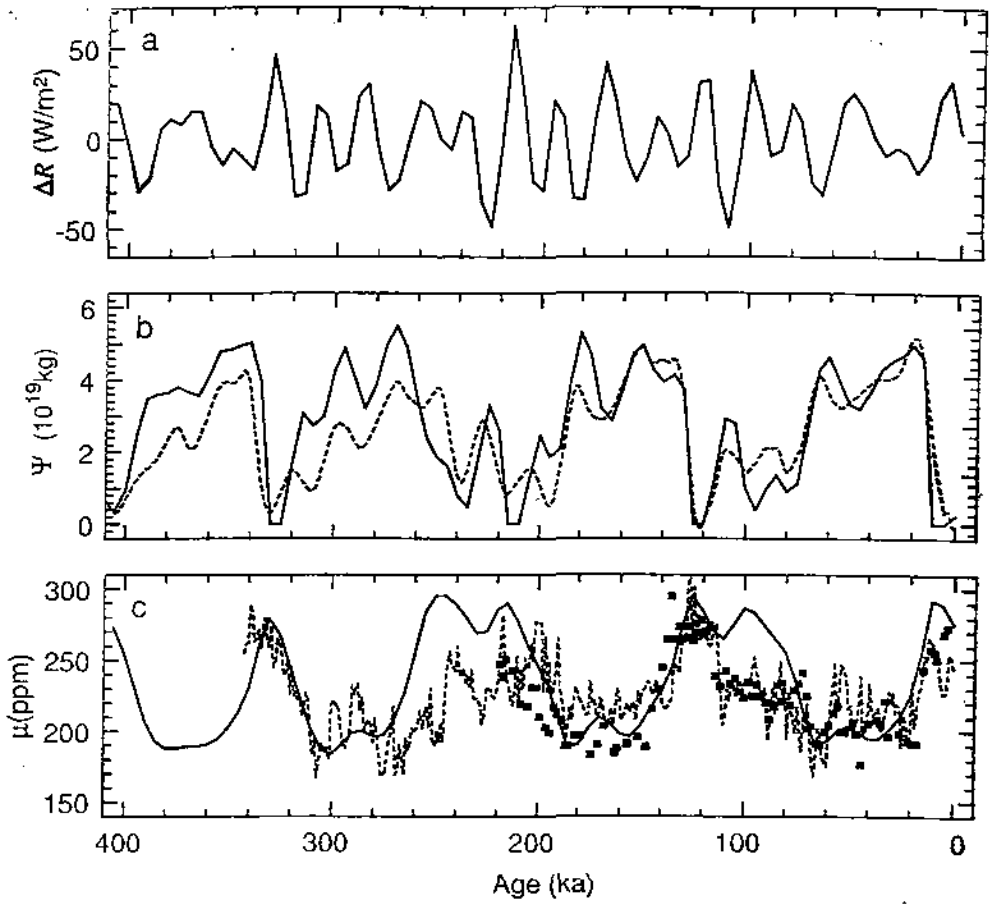

Figure 15-12 (a) Variations of July insolation at 70°N due to Earth-orbital forcing over the past 400 k (b) Expanded view over the past 400 ky of the time-dependent solution for ice mass, Ψ (solid curve compared with the SPECMAP $\delta\,^{18}O$ reconstruction, scaled in terms of ice mass (dashed curve). (c) Time dependent solution for total carbon dioxide μ (solid curve), compared with Vostok CO_2 data of Barnola *et al.* (1987) (squares) and the Shackleton and Pisias (1985) $\delta\,^{13}C$ estimates of CO_2 (dashed curve), which ar scaled to the Vostok data.

9 Models of future climate

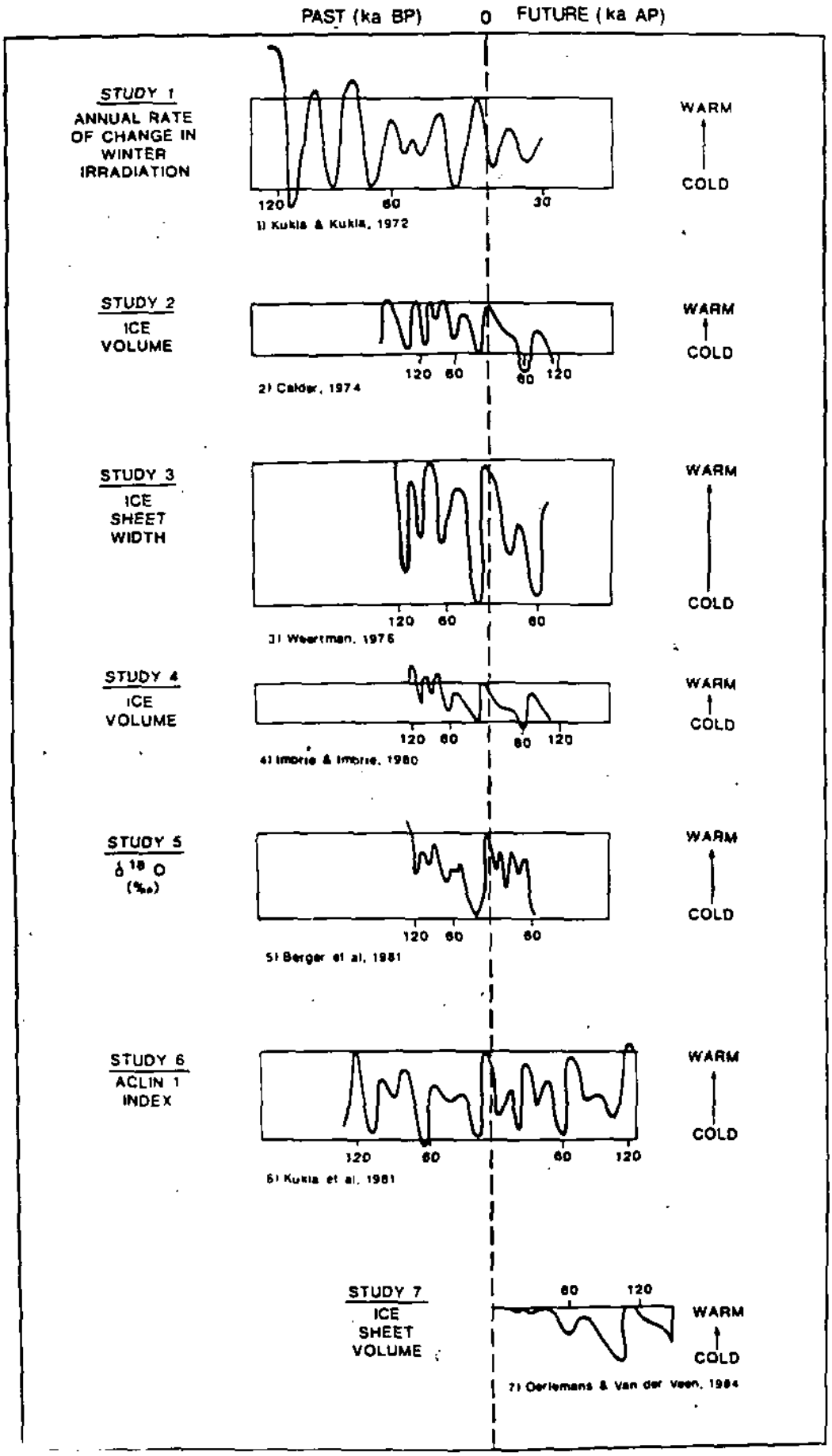

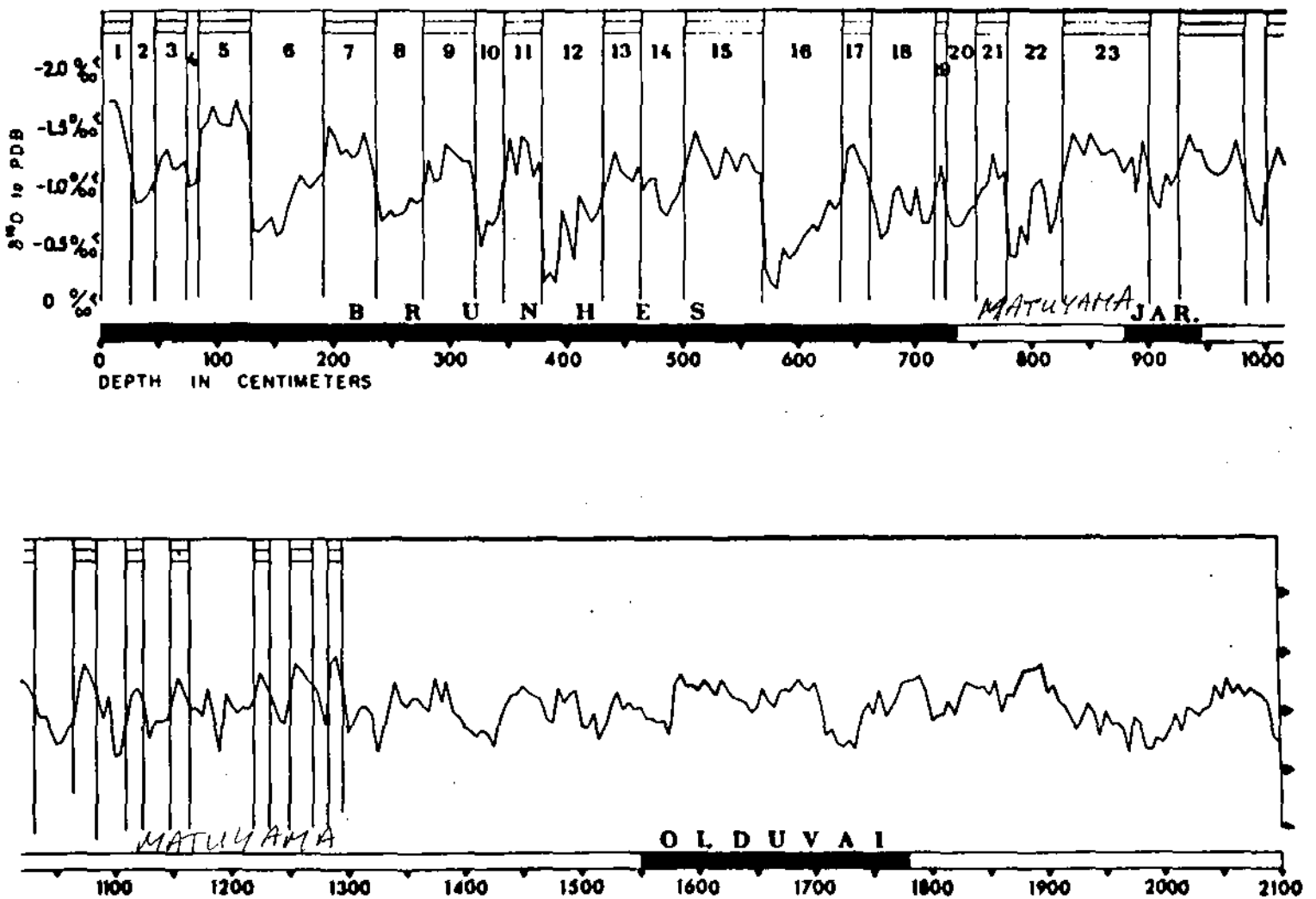

Figure 15. Oxygen-isotopic and paleomagnetic record in upper 880 cm of western equatorial Pacific core V28-239 (location in figure 10). Numbers are oxygen-isotopic stages (after ref. 82).

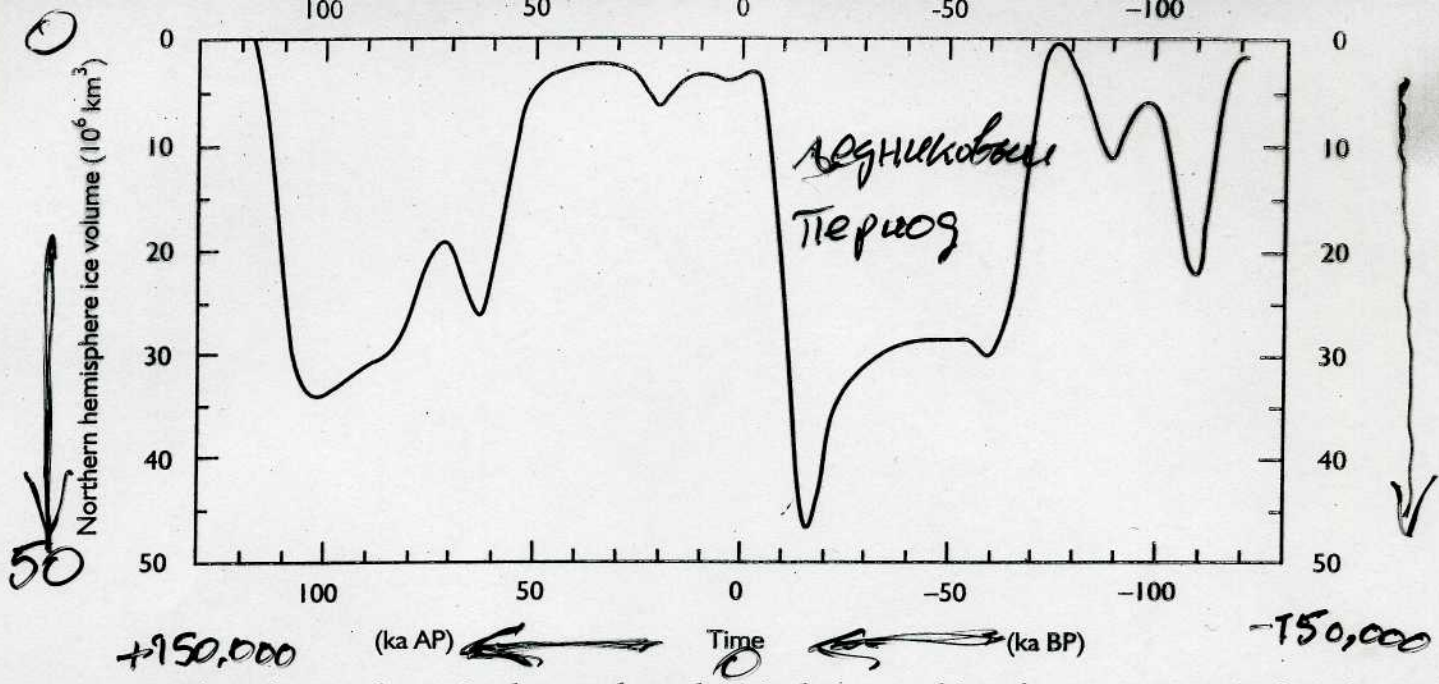

FIGURE 7.1 Predicted ice volume in the northern hemisphere resulting from astronomical and CO_2 forcing. (Modified from Berger and Loutre, 1994)

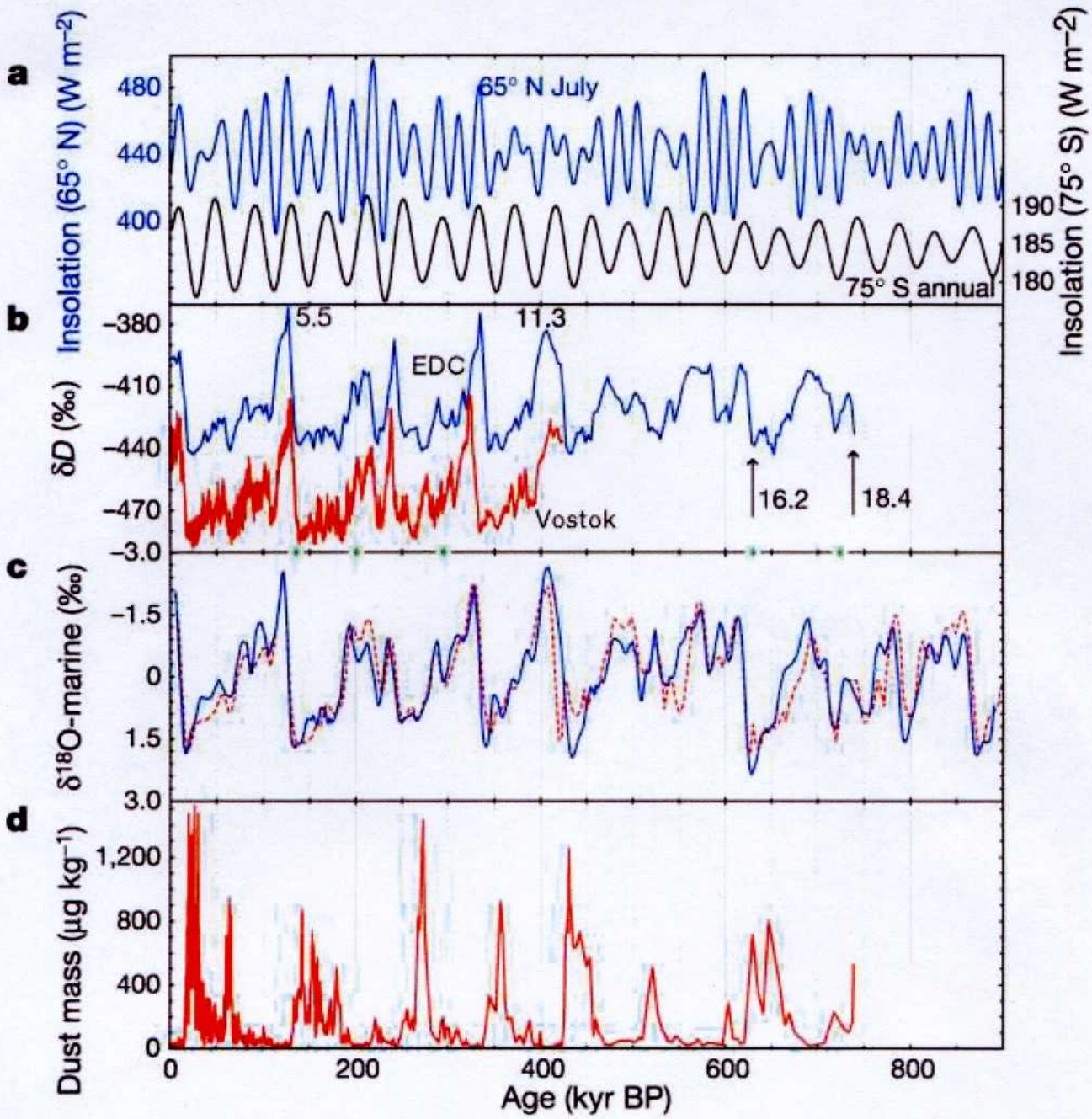

Figure 2.5. a, Insolation records[4]. Upper blue curve (left axis), mid-July insolation at 65° N; lower black curve (right axis), annual mean insolation at 75°S, the latitude of Dome C. **b**, δD from EPICA Dome C (3,000-yr averages). Vostok δD (red) is shown for comparison[1] and some MIS stage numbers are indicated; the locations of the control windows (below 800-m depth) used to make the timescale are shown as

North, G. R., J. G. Mengel, and D. A. Short, A two-dimensional climate model useful in ice age applications, in Milankovitch and Climate, Part 2, A. I- Berger et al., eds., D. Reidel Publ. Co., 1984, 513-518.

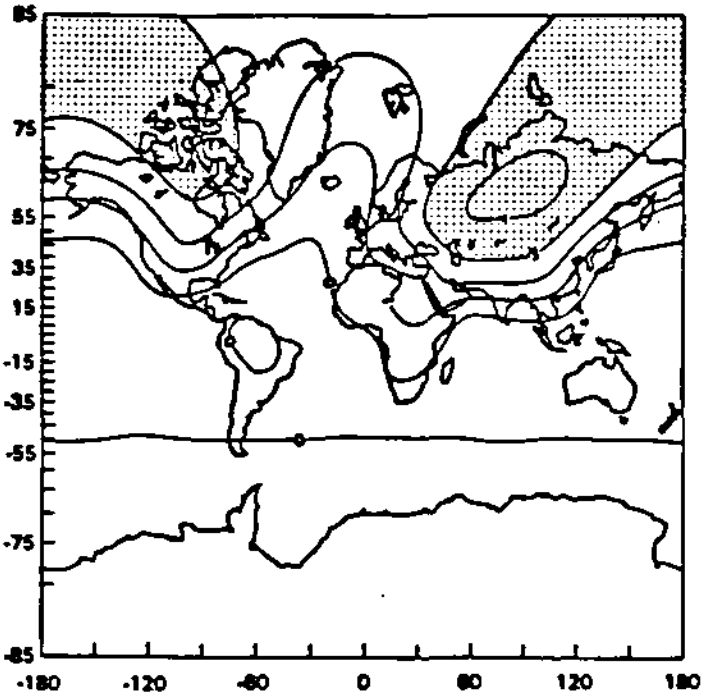

Figure 1. Difference map. Present July minus cool summer orbit July for the linear model. Values greater than 3°C are stippled.

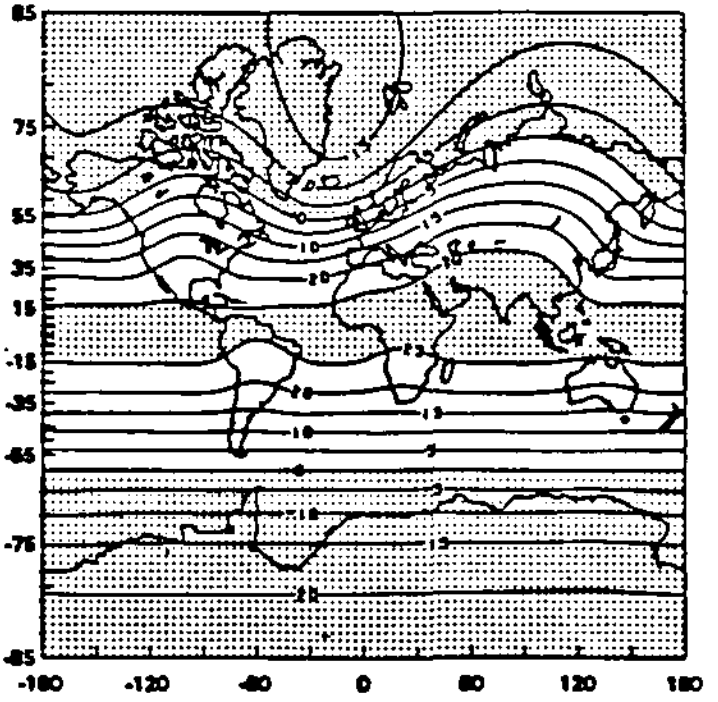

Figure 2. Ice-feedback model July temperature field (°C) for the cool summer orbit. Values less than zero and greater than 25 are stippled. The model infers perennial ice-sheets poleward of the 0°C line in the Northern Hemisphere.

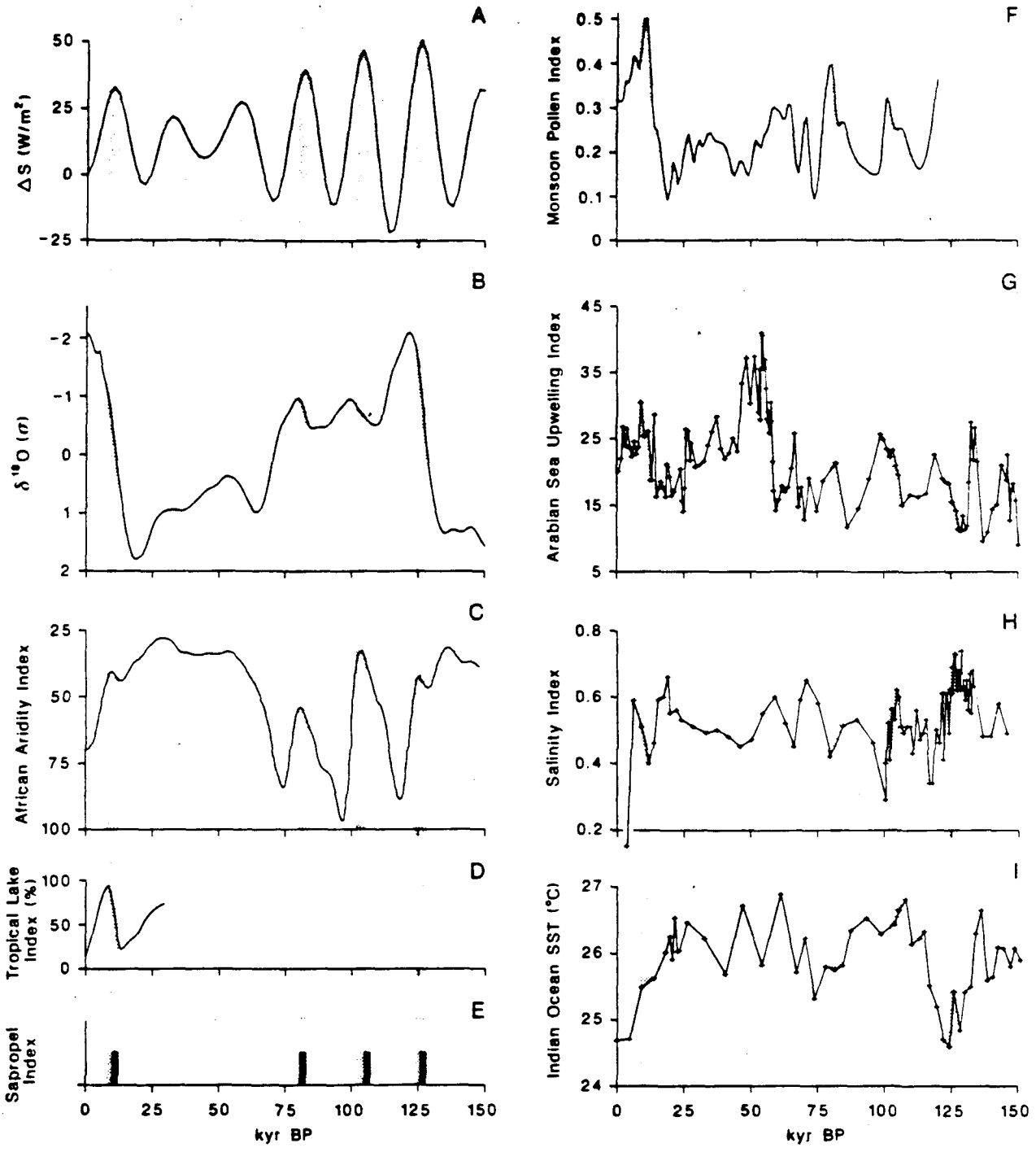

Fig. 2. Comparison of monsoon-related paleoclimatic records with (*a*) average northern hemisphere summer radiation and (*b*) the SPECMAP composite $\delta^{18}O$ record from *Imbrie et al.* [1984] for the past 150 kyr. (*c*) The record of African aridity based upon *Melosira* abundance and indicating wet-dry periods in equatorial Africa, is from *Pokras and Mix* [1985]. (*d*) The tropical lake level record, indicating the percentage of lakes in the intertropical zone that are at high or intermediate levels, is from *Street-Perrott and Harrison* [1984]. (*e*) The Mediterranean sapropel index, indicating presence (vertical bars) or absence of sapropels, is from *Rossignol-Strick* [1983]. (*f*) The record of monsoon-related pollen in the Gulf of Aden is modified from *van Campo* [1982]. (*g*) The faunal record of monsoon-related upwelling off Arabia is from *Prell* [1984]. (*h*) The faunal record of salinity and (*i*) the SST record of the western Indian Ocean are from this work. The times of maximum solar radiation (northern hemisphere average for June–August) are indicated by the shaded vertical bars.

The 100 Ka Cycle (Roe and Miller, GRL, 1999)

USE REGRESSION MODELS BASED ON AR 1 AND 2 PROCESSES FOR LAST 600 Ka.

SUGGEST 6 MODEL OPTIONS:

1. **linear combination of eccentricity e, inclination angle ε and e sin υ (υ = angle between perihelion and vernal equinox)**
2. **inclination angle ε and e sin υ (Muller and McDonald)**
3. **internal oscillation (free)**
4. **internal oscillation - phase locked to ε and e sin υ) (Saltzman and Sutera)**
5. **asymmetric growth/decay of ice from envelope of e sin υ (Imbrie)**
6. **three climate states with transitions related to insolation threshold in high latitudes (Paillard).**

SPECTRAL ANALYSIS OF GLOBAL ICE VOLUME FAILS TO RESOLVE QUESTION.

BETTER EXPLANATION WITH AR2 PROCESS AND WEAK 100 Ka INTERNAL OSCILLATION.

?? WHY/HOW DID OSCILLATIONS START AROUND 750 Ka AGO